

**UC Davis**

**UC Davis Electronic Theses and Dissertations**

**Title**

Evaluating the Impacts of Recycled Water Reuse on Soil Hydrology and Plant Growth

**Permalink**

<https://escholarship.org/uc/item/9tw532qc>

**Author**

Aldughaishi, Usama

**Publication Date**

2023

Peer reviewed|Thesis/dissertation

Evaluating the Impacts of Recycled Water Reuse on Soil Hydrology and Plant Growth

By

USAMA ALDUGHAISHI  
DISSERTATION

Submitted in partial satisfaction of the requirements for the degree of

DOCTOR OF PHILOSOPHY

in

Hydrologic Sciences

in the

OFFICE OF GRADUATE STUDIES

of the

UNIVERSITY OF CALIFORNIA

DAVIS

Approved:

---

Isaya Kisekka, Chair

---

Majdi Abou Najm

---

Mallika Arudi Nocco

Committee in Charge

2023

## Acknowledgements

All praise is due to ALLAH.

In this section, I wish to extend my gratitude to the individuals and organizations who have been supporting and guiding me throughout my studies. First and foremost, I express my sincere appreciation to my supervisor, Isaya Kisekka, for his guidance and support throughout my study. I am also grateful to my esteemed research committee members—Majdi Abou Najm, Mallika Arudi Nocco, Mark Grismer, Jan Hopmans and Daniel Putnam—for their invaluable support and expert advice. Special thanks go to Steve Grattan, Tibin Zhang, Belinda Platts and Michael Cahn for their assistance. I express my sincere appreciation to the dedicated individuals of the Irrigation Management and Agricultural Hydrology Lab (Kisekka Lab) for their collaboration over the years: Umair Gull, Iael Rajj-Hoffman, Felix Ogunmokon, Srinivasa Rao Peddinti, Cassandra Bonfil, Floyd Nicolas, Ian Gomez and Jacob Mueller. My gratitude extends to the following organizations whose funding support made this research possible: Ministry of Higher Education, Oman; Sultan Qaboos University, Oman; Water Research Foundation; and Lassen Canyon Nursery.

Last but certainly not least, I want to express my gratitude to my family and friends. To my parents, even if my entire dissertation were dedicated solely to expressing my gratitude to you, it would not satisfy the dept of gratitude I owe you for everything you have done for me. To my beloved wife and children, you bring joy and meaning to each day. To my siblings, your presence enriches my life. To my extended family and friends, thank you all for being a part of my journey. May ALLAH reward you all.

## Abstract

Clearly, there is a growing demand for freshwater. The agricultural sector accounts for the largest share of freshwater usage, with 70 percent of the total worldwide freshwater. Recycled water reuse for irrigation purposes can serve as an alternative water supply to sustain agricultural production for the growing population. However, the utilization of recycled water can potentially lead to increased land salinity, specific ion toxicity and sodicity where sodicity is directly linked to infiltration issues. In the context of irrigation practices, the assessment of infiltration rates typically relies on both the sodium adsorption ratio (SAR) standard and the salinity of the irrigation water. SAR is commonly employed to estimate changes in infiltration rates when the water is primarily dominated by sodium cations. Nonetheless, recent research findings have indicated that the cation ratio of soil structural stability (CROSS<sub>f</sub>) provides better predictive capabilities for both soil structure and threshold electrolyte concentration compared to SAR especially when the water contains a mixture of both potassium and sodium cations.

Accurate assessment of the potential soil infiltration rate changes and possible soil structure stability alteration is vital to ensuring the sustainable use of recycled water, treated wastewater and low-quality water use in irrigation. In this study, synthetic recycled water was prepared using sodium chloride, potassium chloride, calcium chloride, calcium sulfate (gypsum) and magnesium chloride to prepare treatments with 1.5 dS/m electrical conductivity. Then, SAR and CROSS were evaluated using soil columns and a greenhouse experiment using clay loam soil for both experiments.

For the soil column experiment, 30-columns were conducted. The columns were subjected to evaluation for soil structure and saturated hydraulic conductivity. The irrigation

process involved applying water to soil columns under a continuous 1 cm water head following pre-saturation. The salinity level of the applied solution was consistently maintained at 1.5 dS/m. The results demonstrated a strong correlation between  $CROSS_f$  and both saturated hydraulic conductivity and soil aggregate stability (measured as clay dispersion) in comparison to SAR. The coefficient of determination ( $R^2$ ) for hydraulic conductivity and soil aggregate stability was recorded 0.90 and 0.94 for  $CROSS_f$ , whereas for SAR, these values were 0.75 and 0.78, respectively. Additionally, clay dispersion was evaluated over the depths of the soil column. We found that the treatments that have 0-SAR values but contain potassium in their solutions have significantly more dispersible clay than the calcium chloride treatments for the entire soil column.

For the greenhouse experiment, a total of 11 solution treatments with EC of 1.5 dS/m were prepared. The SAR treatments included 0, 4.9, 9.8 and infinity. The same treatments had  $CROSS_f$  values ranging from 0 to 12.6 and one infinity  $CROSS_f$ . The analyses of the results were divided into two sections. For the first part, the soil structure degradation was evaluated by a permeability test, an infiltration test using Wooding Infiltrometer, soil moisture content using a TDR sensor and clay dispersion using Spontaneous Dispersible Clay Method. The results of the average infiltration relative rates showed an  $R^2$  of 0.20 and 0.60 with respect to SAR and  $CROSS_f$ , respectively. The infinity SAR treatment had the lowest average infiltration rate. The infiltration rate decreased with increasing SAR and  $CROSS_f$ , however,  $CROSS_f$  predicted infiltration reduction better than SAR. Moreover, the average moisture content measured after 7 days of terminating the irrigation slightly increased with increasing  $CROSS_f$  and SAR with  $R^2$  of 0.63 and 0.44 respectively. The infinity SAR or  $CROSS_f$  treatments had the highest soil moisture

content. The moisture content analysis indicates that degraded soil held water for longer periods than aggregated soils.

Strawberry growth and development under recycled water irrigation was evaluated in a greenhouse experiment. The objective was to evaluate the correlation between plant growth and development to SAR and  $CROSS_f$ . The cationic composition in the plant and the sugar content of the fruit were also measured.  $CROSS_f$  had better correlation with both average plant fresh- and dry-biomass with  $R^2$  of 0.6 and 0.5 compared to SAR with  $R^2$  of 0.3 and 0.2, respectively. Additionally,  $CROSS_f$  exhibited a stronger correlation with fruit yield, displaying an  $R^2$  of 0.56 in contrast to SAR's  $R^2$  value of 0.29. Another important finding was that the maximum Na, K, Mg, Ca and Cl that strawberry plants can uptake were determined to be 21, 40, 7.7, 24 and 29 parts per thousand, respectively. Uptake of Na, K, Mg, Ca and Cl from the Osmocote-slow-release fertilizer was 0 (because the fertilizer does not contain sodium), 14, 5.3, 9.1 and 0 parts per thousand, respectively, based on the plant content at the end of the experiment. It was observed that the plant content of magnesium and calcium slightly decreased as the potassium in the irrigation water increased. Additionally, all salts added to the solution was observed in the plant tissue and it was consistent with the respective treatment content.

In both experiments, it was concluded that  $CROSS_f$  could offer enhanced accuracy and insight into the effect of recycled water reuse for irrigation on soil infiltration rate and soil aggregate stability. Therefore, it could be an appropriate standard for predicting sodicity impacts than SAR. For future work, it was recommended that treatments be designed such that the values of  $CROSS_f$  have more spread at a given SAR. This could improve the statistical analysis. Additionally, it is worth comparing the two models in different soils that have clay mineralogy other than montmorillonite which was the case of the soil used in this study.

## Table of Contents

Acknowledgements.....	ii
Abstract.....	iii
Chapter 1.....	1
Introduction.....	1
Chapter 2.....	9
Assessing cation ratios for predicting the impact of recycled water reuse on infiltration and soil structure using soil column experiment .....	9
2.1. Introduction:.....	9
2.2. Methodology: .....	11
2.2.1. Experimental set up: .....	11
2.2.2. Pressure transducers calibration using calibrated digital manometer:.....	13
2.2.3. Soil structure evaluation: .....	14
2.2.4. Statistical analysis: .....	15
2.3. Results and Discussion:.....	16
2.3.1. Pressure transducers calibration: .....	16
2.3.2. Saturated hydraulic conductivity and drainage rate: .....	18
2.3.3. Soil structure evaluation: .....	23
2.4. Conclusions:.....	29
Chapter 3.....	31
Assessing the impact of recycled water reuse for irrigation on soil hydrology in a greenhouse..	31
3.1. Introduction: .....	31
3.2. Methodology: .....	33
3.2.1. Experimental set up: .....	33
3.2.2. Soil permeability evaluation:.....	36
3.2.3. Relative hydraulic conductivity:.....	36
3.2.4. Soil moisture evaluation: .....	37
3.2.5. Soil structure evaluation by clay dispersion: .....	37
3.2.6. Models for predicting soil permeability hazards from using water of marginal quality: .....	38
3.2.7. Statistical analysis: .....	39
3.3. Results and Discussion:.....	39
3.3.1. Soil permeability evaluation:.....	39
3.3.2. Relative hydraulic conductivity:.....	43

3.3.3. Soil moisture evaluation: .....	44
3.3.4. Dispersed clay: .....	46
3.3.5. Summary of the linear correlation: .....	47
3.4. Conclusions: .....	48
Chapter 4 .....	50
Assessing the impact of cation ratios on strawberry growth and development in a greenhouse ..	50
4.1. Introduction: .....	50
4.2. Methodology: .....	52
4.2.1. Experimental set up: .....	52
4.2.2. Treatment specification: .....	53
4.2.3. Leachate sampling: .....	55
4.2.4. Quantitative and qualitative analysis of the plant growth and production: .....	55
4.2.5. Plant and fruit content analysis: .....	56
4.2.6. Statistical analysis: .....	57
4.3. Results and Discussion: .....	58
4.3.1. Leachate analyses: .....	58
4.3.2. Plant growth based on plant cover: .....	62
4.3.3. Yield analysis: .....	64
4.3.4. Sugar content based on °Brix: .....	68
4.3.5. Biomass and plant cover at the end of the experiment: .....	69
4.3.6. Analysis of the plant content: .....	70
4.4. Conclusions: .....	74
Chapter 5 .....	76
Conclusions and Recommendation .....	76
References .....	79
Appendix .....	83

## Chapter 1

### Introduction

A very high portion of freshwater goes to the agricultural sector. For example, about 80% of California's water supply goes to agriculture (Hanak, 2011). Reusing low-quality waters like treated wastewater for irrigation is an alternative water supply to ensure sustainable agricultural production for the increasing population. Recycled water reuse for irrigation could help overcome groundwater overdraft by reducing agricultural freshwater withdrawals. But recycled water use in agriculture has its challenges.

When using primary or secondary treated wastewater, soil salinity buildup could be significant within a few years of application due to high dissolved salts. For example, soil salinity increased by 123% after only three years of irrigation with secondary treated wastewater in Glen Valley, Australia (Dikinya and Areola, 2010). In California, some southern California recreational fields have switched to irrigate with potable water instead of recycled water due to its high TDS (LaSalle, 2018). Other researchers reported increases in salinity when using primary or secondary treated wastewater (Jahantigh, 2008; Klay et al., 2010; Xu et al., 2010).

Tertiary or advanced treated wastewaters, however, have salinity levels even lower than that of freshwater. They differ from freshwater in terms of the presence of constituents with different ratios. For example, potassium availability is minor in natural water and hence in soils irrigated with that water (Richards, 1954). But, potassium's occurrence in treated wastewater is considerable and varies depending on the source of the wastewater (Arienzo et al., 2009; Chand et al., 2020). Thus, recycled water application has more influence on soil sodicity than freshwater due to the elevated concentration of some constituents such as sodium and potassium (Sposito et al., 2016). Usually, freshwater have salts with cations and anions in the following order

Ca $\geq$ Mg $>$ Na and HCO<sub>3</sub> $>$ Cl $\geq$ SO<sub>4</sub> while low-quality waters salts are in the reverse order with Na $\geq$ Mg $>$ Ca and Cl $\geq$ SO<sub>4</sub> $>$ HCO<sub>3</sub>. Velasco (2013) used a Scanning Electron Microscope (SEM) to qualitatively determine dispersibility at a micro-scale. Marchuk et al. (2012) used micro-CT scanning to evaluate the total porosity of soils treated with chloride solution of Na, K, Ca and Mg. The study showed that total porosity was higher in the following sequence: Ca $>$ Mg $>$ K $>$ Na in treated soil. As a result, the proportion of monovalent cations to divalent cations will affect the infiltration rate which will change depending on the composition of sodium, potassium, calcium and magnesium in the water.

Other important factors that determine the hydraulic properties of the soil matrix are soil texture and structure. Soil texture class can be identified based on the percentage of sand, silt and clay particles from a representative sample (Pettygrove and Asano, 1985). The hydrometer method is one way to estimate particle size distribution. Generally, coarse texture soil drains water faster and retain less water than fine texture soils. Soil structure is the arrangement of soil particles to form aggregates. Larger aggregates enhance soil permeability and aeration and help improve drainage because of the large pores between aggregates. Infiltration rate or hydraulic conductivity (K) is a measure of the rate at which water moves through the soil profile (Pettygrove and Asano, 1985), usually expressed as a unit of depth per time. When the soil is saturated, the rate at which water infiltrates is called saturated hydraulic conductivity (K<sub>s</sub>).

Soil texture is a fixed property, however, soil structure can change due to the chemical composition of the water which triggers mechanisms of flocculation and dispersion. The water's chemical properties influencing soil structure through flocculation and dispersion include water salinity and the cationic content, primarily sodium, potassium, calcium and magnesium. The dispersion and flocculation processes occur mainly due to the interaction of the repulsive and

attractive forces. Both forces can come simultaneously into play. However, depending on the dominant interactive forces, clay particles may disperse if dominant forces are repulsive or flocculate if the dominant forces are attractive (Wallender and Tanji, 1990).

Generally, monovalent cations (like sodium and potassium) can be easily replaced or exchanged by divalent cations (like calcium and magnesium) because monovalent cations are attracted to a single charge. Upon hydration (watering), a layer will coat the clay particles causing diffusive double layer (DDL). The thickness of the positive coating layer depends on the cation type which will determine the diffusive double layer thickness (Hillel, 1998; Wallender and Tanji, 1990). Large monovalent cations neutralize one negative charge (diffuse at a lower rate with distance from the clay surfaces). The net positive layer will be thick causing dispersion to the adjacent particles due to similar charges causing repulsion. Smaller cations (like calcium and magnesium) neutralize more than one negative charge (their equivalent concentration is higher at the clay surface than that of the monovalent cations) and the layer will be thin causing the particles to come closer to each other such that unified positive layer might form between two clay surfaces (platelets). Additionally, swelling and dispersion is influenced by the clay type because of their shape and structure that forms based on the original weathered rock composition (Hillel, 1998). Smectites, for example, show extensive dispersion because of their 2:1 layer structure (Buelow et al., 2015) and because of their strong isomorphous substitution and cation exchange capacity, very weak interlayer bond and high surface area. Kaolinite-rich soils, however, are more stable and have a 1:1 layer (McNeal and Coleman, 1966). Illite and vermiculite soils are also 2:1 layer (like smectites) but they have intermediate dispersion capability.

The commonly used method to assess soil infiltration based on irrigation water quality is the Sodium Adsorption Ratio (SAR), which considers sodium as the primary cation responsible for alkali hazard (Richards, 1954). Recently, parameters analogous to SAR were developed (Table 1.1). All the new parameters included potassium in the model to account for its soil aggregate dispersity.  $CROSS_f$  was found to be a better predictor than SAR for soil structure changes measured as spontaneous dispersible clay with an  $R^2$  value of 0.95. While  $CROSS_{opt}$  demonstrated a high level of prediction accuracy for the threshold electrolyte concentration with an  $R^2$  value of 0.95.

Table 1.1: Models for predicting the impact of irrigation water cation composition on soil hydraulic properties.

Name	Model	Reference
Sodium adsorption ratio	$SAR = \frac{Na^+}{\sqrt{Ca^{2+} + Mg^{2+}}}$	Richards (1954)
Monovalent cation adsorption ratio	$MCAR = \frac{Na^+ + K^+}{\sqrt{Ca^{2+} + Mg^{2+}}}$	(Smiles and Smith, 2004)
Cation ratio of structural stability (based on relative flocculating power)	$CROSS_f = \frac{Na^+ + 0.56 * K^+}{\sqrt{Ca^{2+} + 0.60 * Mg^{2+}}}$	Rengasamy and Marchuk (2011)
Cation ratio of structural stability (based on relative dispersing power)	$CROSS_d = \frac{Na^+ + 0.26 * K^+}{\sqrt{Ca^{2+} + 0.30 * Mg^{2+}}}$	Smith et al. (2015)
Cation ratio of structural stability (optimized)	$CROSS_{opt} = \frac{Na^+ + 0.335 * K^+}{\sqrt{Ca^{2+} + 0.0758 * Mg^{2+}}}$	Smith et al. (2015)

Therefore, accurate soil structure assessment when using low quality waters is necessary to ensure sustainable recycled water reuse for irrigation. SAR could give an initial assessment because of sodium dominance on soil dispersion than potassium. However, considering the long-term application and different effluent sources, SAR alone would not be an appropriate

assessment tool. Due to the predictability of  $CROSS_f$  and  $CROSS_{opt}$ , they were chosen for comparison with the SAR of the treatments. The overall hypothesis is that both soil structure and hydraulic conductivity will degrade as the cation ratios (SAR,  $CROSS_f$  and  $CROSS_{opt}$ ) increase. It is expected that the evaluation of soil structure (measured as spontaneous dispersed clay) will closely correlate with  $CROSS_f$  while hydraulic conductivity will show a stronger correlation with  $CROSS_{opt}$ . The overall purpose of this study is to evaluate the impact of sodium, potassium, calcium and magnesium when they are present in water on soil permeability, soil structure and plant growth.

The following analyses of the models are based on two experiments including soil columns and greenhouse studies. Both experiments employed synthetic recycled water, ensuring precise control over salinity and cation concentration ranges. Field soil characterized by a clay loam texture was utilized in these experiments. The scope of treatments, spanning SAR,  $CROSS_f$  and  $CROSS_{opt}$  values, is depicted in the SAR-EC chart (Ayers and Westcot, 1985) presented in Figure 1.1. It is important to note that a sodium chloride solution was included as another treatment; however, it is not depicted in the figure due to its numerically infinite value.

It is important to note that the greenhouse experiment was conducted before the column experiment. The greenhouse experiment took place between August 2020 and June 2021, while the column experiments were conducted in different sets between May 2022 and May 2023. As can be seen from Figure 1.1, the treatments were designed to have three levels of SAR. The same treatments exhibited varying values in terms of  $CROSS_f$  and even more variation in terms of  $CROSS_{opt}$ . Upon the completion of the greenhouse experiment, it was found that  $CROSS_f$  proved to be a better model than  $CROSS_{opt}$ . Consequently, the treatments were reconfigured for the

column experiment to introduce greater variation in terms of  $CROSS_f$  compared to the greenhouse experiment.

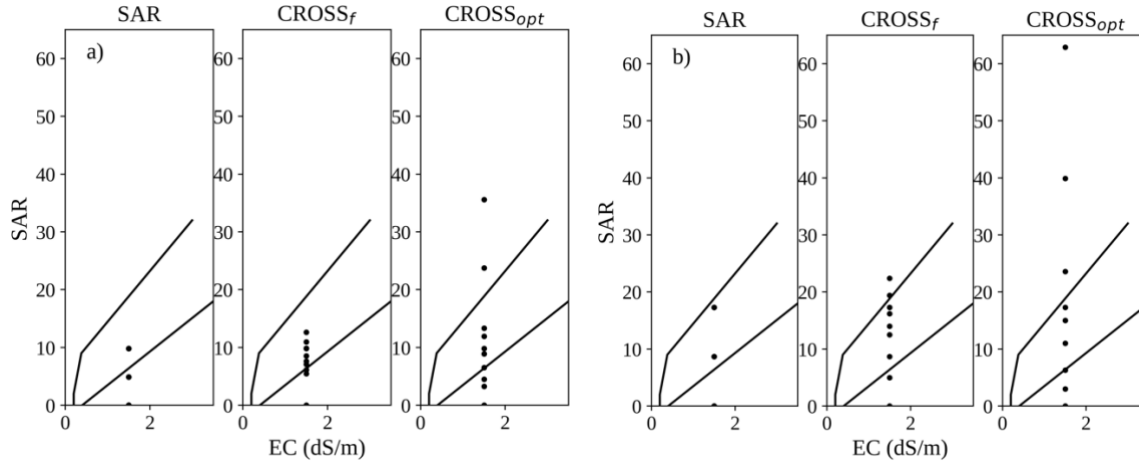


Figure 1.1. Treatments range over the SAR-EC chart (Ayers and Westcot, 1985) where the lines separate the zones of no reduction in infiltration, slight to moderate reduction in infiltration and severe reduction in infiltration rate: a) greenhouse experiment and b) column experiment.

It is important to note that the greenhouse experiment was conducted before the column experiment. The greenhouse experiment took place between August 2020 and June 2021, while the column experiments were conducted in different sets between May 2022 and May 2023. As can be seen from Figure 1.1, the treatments were designed to have three levels of SAR. The same treatments exhibited varying values in terms of  $CROSS_f$  and even more variation in terms of  $CROSS_{opt}$ . Upon the completion of the greenhouse experiment, it was found that  $CROSS_f$  proved to be a better model than  $CROSS_{opt}$ . Consequently, the treatments were reconfigured for the column experiment to introduce greater variation in terms of  $CROSS_f$  compared to the greenhouse experiment.

Chapter 2 presents the analysis of the column experiment. The primary objectives were to assess the impact of using synthetic recycled water on saturated hydraulic conductivity over time and analyze changes in soil structure with increasing depth. Subsequently, the correlation between hydraulic conductivity and soil structure changes with SAR and CROSS were evaluated. Thirty large soil columns, comprising three replications of ten treatments each, were employed for this study. The irrigation process consisted of providing water to the soil columns under a continuous 1 cm water head using a Wooding infiltrometer (Perroux and White, 1988) following pre-saturation.

Chapter 3 presents an analysis of the soil's physical properties within the greenhouse pots. A total of 11 solution treatments, each with an electrical conductivity (EC) of 1.5 dS/m, were prepared. Within each treatment, four replications were incorporated into a complete randomized block design. The SAR treatments encompassed values of 0, 4.9, 9.8 and infinity. Correspondingly, the CROSS<sub>f</sub> values for the same treatments ranged from 0 to 12.6, with one instance of infinity for CROSS<sub>f</sub>. Drip irrigation was used for irrigation and MixRite fertilizer injectors were utilized to inject concentrated treatment solutions into the irrigation line resulting in a conductivity of 1.5 dS/m. The assessment of soil structure degradation involved a permeability test, an infiltration test utilizing the Wooding Infiltrometer, measurements of soil moisture content using TDR sensors and an evaluation of clay dispersion via the Spontaneous Dispersible Clay Method.

Chapter 4 presents an analysis of strawberry growth and development within a controlled greenhouse environment using pots filled with clay loam soil. The main objective of the study was to assess the correlation between plant growth and development with SAR and CROSS values. The growth and development of strawberries were evaluated based on several factors,

such as yield over the growth period, sugar content as measured by °Brix, plant growth as measured by plant cover, biomass at the end of the growth period, plant ion uptake and leachate analysis. Additionally, cation ratios were examined to establish any correlations with growth, yield and biomass.

Finally, Chapter 5 synthesizes major findings from soil column and greenhouse studies evaluating the impact of recycled water reuse for irrigation on soil hydrology and strawberry growth and development. A comparative analysis was conducted between the main findings of the column experiment and those of the greenhouse experiment. The primary distinction between the two experiments lies in the method of water supply. The column experiment utilized a continuous 1-cm water head supply, whereas the greenhouse experiment employed drip irrigation. Additionally, the greenhouse experiment featured the influence of strawberry plant roots and incorporated the use of slow-release fertilizer to bolster plant growth. Consequently, the analysis of cation ratios was examined under two conditions: with no plants and with plant conditions. The consistency of results obtained from the two separate studies supports the overall conclusions drawn from the research that  $CROSS_f$  could be a better replacement than SAR.

## Chapter 2

### Assessing cation ratios for predicting the impact of recycled water reuse on infiltration and soil structure using soil column experiment

#### 2.1. Introduction:

Soil salinity, clay dispersion and clay expansion are significant issues for modern agriculture (Hailu and Mehari, 2021; Rengasamy, 2010). Soil salinity reduces crop yield and degrades soil quality (Cuevas et al., 2019; Haj-Amor et al., 2022), whereas clay dispersion and swelling have a negative impact on soil structure, water infiltration and root development (Amezketta et al., 2004; Rengasamy, 2018). As a result, these problems impede agricultural productivity and threaten global food security. In order to address these challenges and develop appropriate mitigation strategies, a comprehension of the complex interaction between soil properties, water resources and land management practices is required (Thaker et al., 2021). In addition, interdisciplinary research is crucial for identifying innovative solutions that can improve soil health, increase agricultural productivity and promote sustainable farming practices (Hou et al., 2020).

Reusing recycled water for irrigation is a viable strategy for promoting sustainable agricultural production and reducing groundwater overdrafts by decreasing agricultural withdrawals (Jaramillo and Restrepo, 2017; Jeong et al., 2020). Utilizing treated effluent for irrigation conserves water resources while maintaining crop yields and ensuring food security (Lahlou et al., 2020). This strategy has gained increasing attention in recent years due to the rising demand for water resources and the emphasis on sustainable solutions (Hashem and Qi, 2021; Vergine et al., 2017). In addition, using recycled water for irrigation reduces the environmental impact of agricultural production and promotes the implementation of circular

economy principles in the agricultural sector (Hagenvoort et al., 2019). Integrating these practices into modern agricultural systems requires effective policies, sophisticated treatment technologies and ongoing monitoring of potential environmental and health risks related to wastewater reuse.

Recycled water use in agriculture has its challenges. Although tertiary or advanced treated wastewaters have reported lower salinity levels than freshwater, the difference in present constituents can significantly impact soil structure. Thus, the application of recycled water can have a greater influence on soil sodicity than freshwater (Sposito et al., 2016). In particular, potassium levels are often insignificant in natural waters (Richards, 1954), but its occurrence in treated wastewater is considerable and varies depending on the source of the wastewater (Arienzo et al., 2009; Chand et al., 2020). Potassium has been reported to have a negative impact on soil permeability (Ahmed et al., 1969; Arienzo et al., 2009; Chand et al., 2020; Chen et al., 1983; Martin and Richards, 1959; Quirk and Schofield, 1955; Reeve et al., 1954; Rengasamy and Marchuk, 2011; Smith et al., 2015). In some instances, soil aggregates have shown better stability in potassium-saturated soils than in calcium or magnesium saturated soils (Cecconi et al., 1963; Chen et al., 1983; Ravina, 1973).

Irrigation water quality is traditionally assessed using the Sodium Adsorption Ratio (SAR), (Richards, 1954), where sodium is weighted as the major cation responsible for soil sodicity. Notably, potassium isn't accounted for in the SAR. To better account for the soil dispersive powers of both sodium and potassium while accounting for the flocculating effects of magnesium and calcium, researchers Rengasamy and Marchuk (2011) developed the Cation Ratio of Soil Structural Stability (CROSS). Smith et al. (2015) further optimized CROSS to have better predictivity of clay dispersion using their experimental data. When considering the long-

term application of recycled water, SAR alone would not be a sufficient assessment tool. Column experiments are widely used to study soil infiltration, especially to verify a particular model or relation (Yang et al., 2004). They offer better control compared to field studies.

Therefore, the overall purpose of this study was to evaluate the effect of synthetic recycled water use on soil saturated hydraulic conductivity and changes in soil structure with increasing depth using soil columns. The synthetic recycled water was made of chloride solutions of sodium, potassium, calcium and/or magnesium. Thus, the correlation between hydraulic conductivity and soil structure changes with Sodium Adsorption Ratio and Cation Ratio of Structural Stability was then evaluated.

## 2.2. Methodology:

### 2.2.1. Experimental set up:

Acrylic columns (14.7 cm diameter x 60 cm tall) were used. Each column was carefully packed with sieved (6mm) homogenized Yolo Clay Loam soil collected from the University of California Davis farm near Davis CA. The effective soil depth inside the columns was 53 cm as there was an initial 3 cm layer of glass beads at the bottom of the column and a 4 cm clearance at the top of the column for the infiltrometer. The soil was packed in increments of 5 cm to an average bulk density of  $1.3 \text{ g/cm}^3$ . Since the soil was air dried, the initial moisture content of the soil was estimated to correct the weight to have a bulk density of  $1.3 \text{ g/cm}^3$ . The top surface of each layer was shattered to lessen the boundary compaction. The initial soil physical and chemical properties are listed in Table 2.1.

Table 2.1: Properties of the soil used in the experiment to study the effect of recycled water reuse on soil permeability and soil structure.

Parameter (unit)	Average value (standard deviation)	Method/tool
EC <sub>e</sub> (dS/m)	0.95 (±0.06)	Saturated paste extract
pH	7.1 (±0.53)	Saturated paste extract
sand (%)	35.06 (±0.86)	Hydrometer method
silt (%)	31.56 (±1.73)	Hydrometer method
clay (%)	33.38% (±1.25)	Hydrometer method
gravel (%)	0.06% (±0.06)	Gravimetric (scale)
texture	clay loam	Soil texture triangle
field BD (g/cm <sup>3</sup> )	1.33 (±0.09)	Core sample
organic carbon	1.26 (±0.08)	Loss-on-ignition
Exchangeable Na (meq/100g)	0.13 (±0.01)	ICP-AES
Exchangeable K (meq/100g)	0.83 (±0.07)	ICP-AES
Exchangeable Ca (meq/100g)	8.27 (±0.25)	ICP-AES
Exchangeable Mg (meq/100g)	11.83 (±0.32)	ICP-AES
CEC (meq/100g)	21.1 (±0.53)	Measured
ESP (%)	0.60 (±0.53)	Measured
dominant clay mineral	Montmorillonite	From literature <sup>1</sup>

<sup>1</sup> From Dasberg and Hopmans (1992) and Lagerwerff and Brower (1972)

Each soil column received prepared synthetic recycled water with a salinity of approximately 1.5 dS/m (Table 2.2) from the top using a Wooding Infiltrometer (an equivalent constant-head permeameter device that relies on a Mariotte siphon). Therefore, a total of 30 soil column experiments were conducted with three replications per treatment. The soil columns were pre-saturated from bottom to top using tap water ensuring a uniformly saturated starting condition for all the soil columns. The water was allowed to infiltrate freely and a continuous water supply was maintained throughout the experiment. The infiltrometer used was designed to keep a constant 1 cm water head above the soil surface. It was assumed that the soil near the top of the column is fully saturated implying a unit hydraulic gradient. As a result, the saturated hydraulic conductivity ( $K_{sat}$ ) was equated to the infiltration rate. The estimation of soil saturated hydraulic conductivity was carried out for each soil column across the application of solution treatments spanning a pore volume (which is the volume of the total pore spaces of the soil in the

column). On average, approximately 4 L of water were utilized to saturate the columns with an average wetting rate of 2.0 mm/h. Consequently, a water application of 4 L was considered equivalent to one pore volume. The drainage water was collected at the bottom of each column into a bucket to estimate the average outflow rates for each pore volume application.

Table 2.2: Synthetic recycled water treatments specification.

Treatments	T0	T1	T2	T3	T4	T5	T6	T7	T8	T9
EC (dS/m)	1.5	1.5	1.5	1.5	1.5	1.5	1.5	1.5	1.5	1.5
NaCl (mmol/L)	0	16	15	15	15	7.5	7.5	7.5	0	0
KCl (mmol/L)	0	0	0	0	0	6	6	6	11	12
CaCl <sub>2</sub> (mmol/L)	8	0	0.75	0.375	0	0.75	0.375	0	1.5	0.375
MgCl <sub>2</sub> (mmol/L)	0	0	0	0.375	0.75	0	0.375	0.75	0	0.375
SAR	0	∞	17.3	17.3	17.3	8.7	8.7	8.7	0	0
CROSS <sub>f</sub>	0	∞	17.3	19.4	22.4	12.5	14.0	16.2	5.0	8.7
CROSS <sub>opt</sub>	0	∞	17.3	23.6	62.9	11.0	15.0	39.9	3.0	6.3

### 2.2.2. Pressure transducers calibration using calibrated digital manometer:

The water level in the Mariotte tower was measured manually as well as using a pressure transducer. The pressure transducer was linked to a CR 1000 Datalogger, allowing for data collection to be automated. The water level readings were collected at regular intervals by the Datalogger, making it easy to examine the data over time. The pressure transducers were calibrated with a digital manometer to assure precise measurements. The manometer was set to measure in centimeters of water (cm H<sub>2</sub>O). Calibration was required to guarantee that the transducers' measurements match the real water levels. The CR 1000 Datalogger was used to translate the voltage data from the pressure transducers into pressure units, namely kilopascals (kPa). This conversion made it possible to provide the recorded data in a standardized unit for easier analysis and comparison. The Datalogger was programmed to output the converted

pressure data at 15-minute intervals. This frequency of data collection enables extensive observation and study of water level fluctuations throughout time. The recorded data from the Datalogger was compared with the manually recorded infiltration rate to examine the accuracy and dependability of the pressure transducers. The accuracy with which the pressure transducers predicted the water level inside the infiltrometer can be evaluated by comparing the two sets of data.

### 2.2.3. Soil structure evaluation:

A laser scattering particle size distribution analyzer (Partica LA-960V2, HORIBA, Ltd.) was used to determine the particle size distributions (PSDs) of treatments T0 (calcium chloride solution) and T1 (sodium chloride solution). Representative soil samples from the top 1 cm of the soil columns were collected after terminating the infiltration test and deionized water was incrementally added and mixed to each soil sample until the mixture resembled a saturated paste (Rhoades, 1982) and stored overnight. Approximately 0.1 to 0.5 g of each paste was fed into the analyzer for wet dispersion. The particle analyzer was automated for two different procedures, one including circulation and one including agitation and circulation. For both procedures, an average of three PSDs were collected at different times over 2 hours.

To comprehensively compare all treatments, a thorough assessment of soil structure changes was conducted at various depths upon the end of the experiment. The evaluation employed the spontaneous dispersible clay method outlined in Marchuk et al. (2013). Soil samples were collected from the soil columns from the topmost 1 cm, the 0-10 cm layer (reported as 5cm), the 20-30 layer (reported as 25cm) and the 40-50 cm layer (reported as 45cm). A total of 120 samples were analyzed. For the analysis, 40 g of the oven-dried samples were

utilized to estimate the quantity of dispersed clay. The samples were placed in 250-ml-graduated cylinders into which 200 ml of deionized water was gradually added. The solutions were allowed to stand for a duration of 5 hours before initiating the suspension of the soil. After a subsequent 2-hour interval, a 10 ml subsample was extracted from the bulk solution at a depth of 10 cm beneath the surface. The 10 ml subsample was oven-dried and subsequently weighed using a sensitive scale with an accuracy of  $\pm 0.1$  mg.

#### 2.2.4. Statistical analysis:

The sodium adsorption ratio (SAR) is a commonly used indicator of soil infiltration changes based on the salinity of the irrigation water (Richards, 1954):

$$SAR = \frac{Na^+}{\sqrt{Ca^{2+} + Mg^{2+}}} \quad 2.1$$

where the ions' concentrations are in mmol/L. The cation ratio of soil structural stability (CROSS) was suggested by Rengasamy and Marchuk (2011) to consider the effect of potassium on soil structure stability:

$$CROSS_f = \frac{Na^+ + 0.56 * K^+}{\sqrt{Ca^{2+} + 0.60 * Mg^{2+}}} \quad 2.2$$

the  $f$  subscript indicates that the potassium and magnesium factors are based on the flocculating power relative to sodium and calcium, respectively. Equation 2 predicts clay dispersion more accurately than SAR with  $R^2$  of 0.95 (Rengasamy and Marchuk, 2011). Using experimental data on threshold electrolyte concentration (TEC) from Arienzo et al. (2012), Smith et al. (2015) further improved equation 2 to provide best-fit-factors lower than one for potassium and magnesium. The outcome was:

$$CROSS_{opt} = \frac{Na^+ + 0.335 * K^+}{\sqrt{Ca^{2+} + 0.0758 * Mg^{2+}}} \quad 2.3$$

where the *opt* subscript denotes optimization. The optimized equation was found better predictor for the TEC than Equation 1 and 2 with  $R^2$  of 0.95.

A linear regression test was conducted to evaluate the Equations 1, 2 and 3 with respect to the means of the infiltration rate measured at the pore volume 8 and the average spontaneous clay dispersion of the top 1 cm samples. Root means square error (RMSE) and  $R^2$  were used to assess the calibration and the performance of the pressure transducers attached with the infiltrometer. The means of treatments output results were compared using Tukey-Kramer's HSD test at a significance level of 5%. The normality of the data distribution was verified before the means were separated. All analyzed data satisfied this requirement, except for the saturated hydraulic conductivity, which had to be log-transformed before the means were separated. However, the actual values are presented in the results.

## 2.3. Results and Discussion:

### 2.3.1. Pressure transducers calibration:

In the experiment, 5 infiltrometers were used, each equipped with a pressure transducer to detect water levels. All of the pressure transducers were calibrated and 11 data points were recorded for each transducer. Given that the maximum water level inside the infiltrometer was 80 cm, the data collecting range was 0 to 100 cm of water. For each pressure transducer, the calibration method required recording the observed manometer readings as well as the related datalogger output. Figure 2.1 depicts the calibration results, which show the link between the sensor readings and the actual water levels inside the infiltrometer. Notably, the calibration equation has a high coefficient of determination, close to one, indicating a strong correlation between sensor data and actual water levels. Furthermore, the calibration equation's root mean

square error (RMSE) was approximately 1.924, reflecting a relatively small average variation between predicted and actual results.

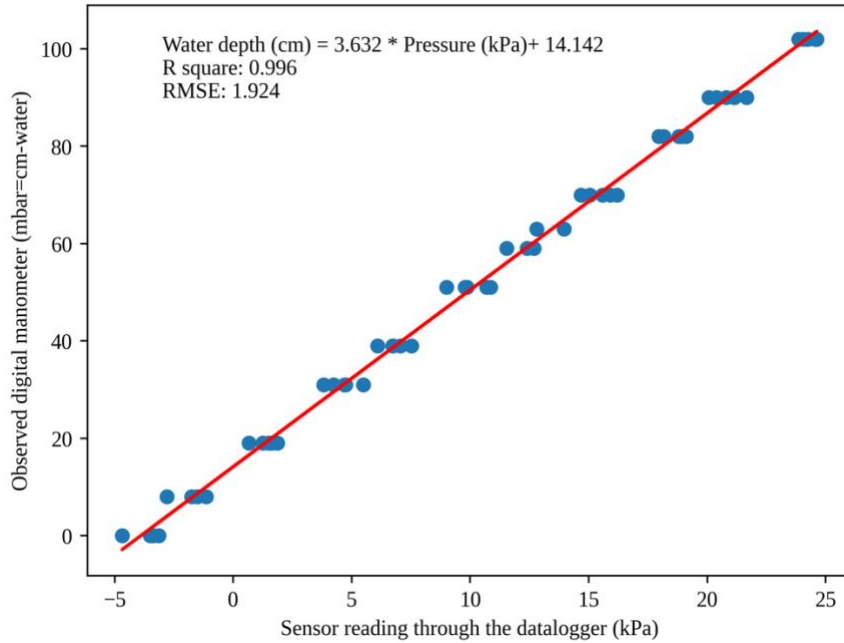


Figure 2.1: Calibration of the pressure transducers attached to the Wooding infiltrometer and connected to the datalogger.

Because the infiltrometer's diameter was 7 cm and the soil column's diameter was 14.7 cm, a conversion factor of 0.227 was multiplied to the output water level values to precisely determine the actual water depth infiltrated into the soil. Figure 2.2 depicts the pressure transducers' performance in predicting saturated hydraulic conductivity. The results showed a well-fitted 1:1 relationship between recorded saturation infiltration rates (ranging from 0.23 to 8.55 ml/min) and measured saturated hydraulic conductivity (ranging from 0.001 to 0.050 cm/min). This alignment verifies the sensors' precision and accuracy in predicting water levels within the infiltrometer. The sensors' high prediction capabilities are further supported by the

coefficient of determination ( $R^2$ ) of 1 and zero RMSE, demonstrating a perfect fit between the expected and actual readings.

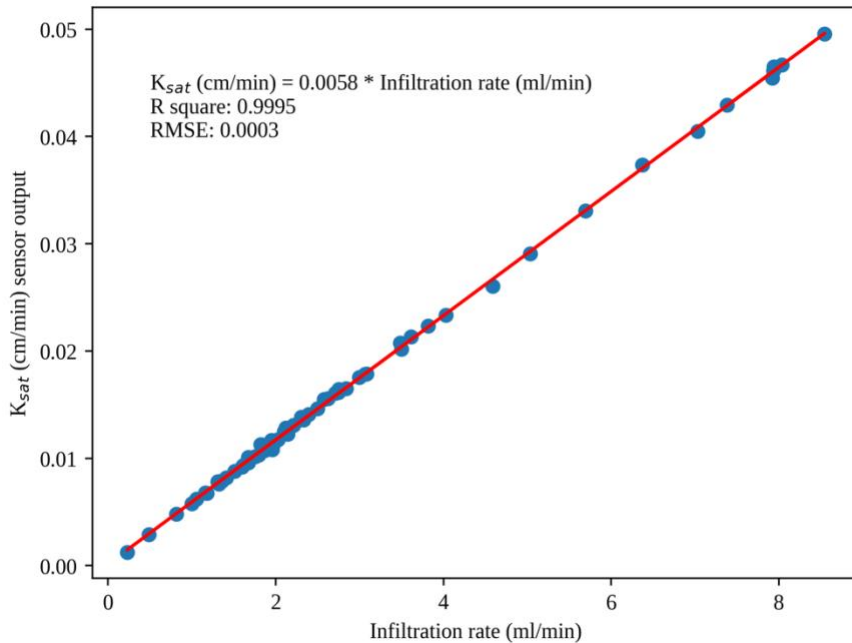


Figure 2.2: Performance of the pressure transducers in predicting the water depth in the Wooding Infiltrometer connected to the infiltrometer.

### 2.3.2. Saturated hydraulic conductivity and drainage rate:

Figure 2.3 depicts the progression of the average saturated infiltration rate in relation to the pore volume application of the treatment solution. The curves are encompassed by shaded areas representing the standard error associated with each data point. Data points lacking shaded areas correspond to either an average of two measurements or a single measurement. Across most treatments, there was a marginal decline in the saturated infiltration rate up to pore volume 3 followed by a subsequent increase in the infiltration rate. The initial reduction in the infiltration rate could potentially be attributed to hysteresis resulting from the bottom-up pre-saturation of the soil column as well as the occurrence of preferential flow. For the preferential flow, the flow

paths of water might change as it goes from top to bottom until it has the fastest path that leads to the bottom of the soil.

Table 2.3 presents the outcomes of the Tukey-Kramer's HSD test. Evidently, treatment T0 (calcium chloride solution) displayed noteworthy statistical significance when compared to the other treatments. The application of this treatment solution led to a marked enhancement in the infiltration rate across the entire measurement span. The increasing infiltration rate of this treatment allowed it to achieve a 16-pore volume run. The primary objective was to ascertain the maximum steady state infiltration rate, yet this determination proved elusive even after 16 pore volume applications. Treatments T8 and T9 had SAR values of zero and they were both statistically lower than T0. The comparatively slow infiltration rate of the T8 and T9 can primarily be attributed to the influence of potassium on infiltration rate given that these treatments encompassed potassium, calcium and/or magnesium. Throughout the entire experiment, T8 maintained a higher average infiltration rate than T9 which could potentially be attributed to calcium's more pronounced effect on aggregate flocculation in comparison to magnesium, as T8 lacked magnesium in its solution whereas T9 incorporated magnesium.

The lowest observed average saturated infiltration rate was associated with treatment T1 although this disparity did not reach statistical significance when compared to treatments T3 and T4. In contrast, treatment T2 exhibited a similar SAR to T3 and T4 yet it demonstrated statistical significance over treatment T1. On average, T2 displayed a higher infiltration rate in comparison to T3 and T4. This divergence may arise from varying degrees of calcium's and magnesium's impact on aggregate flocculation as T2 had calcium alongside sodium and potassium cations. Additionally, treatment T2 did not reach a constant infiltration rate after the application of 10 pore volume of its solution. Despite treatment T3 having a smaller  $CROSS_f$  value compared to

T4, its average infiltration rate from pore volume 5 to pore volume 8 fell below that of T4.

Notably, no statistically significant distinctions emerged within the group of treatments featuring an SAR of 8.7 (T5, T6 and T7).

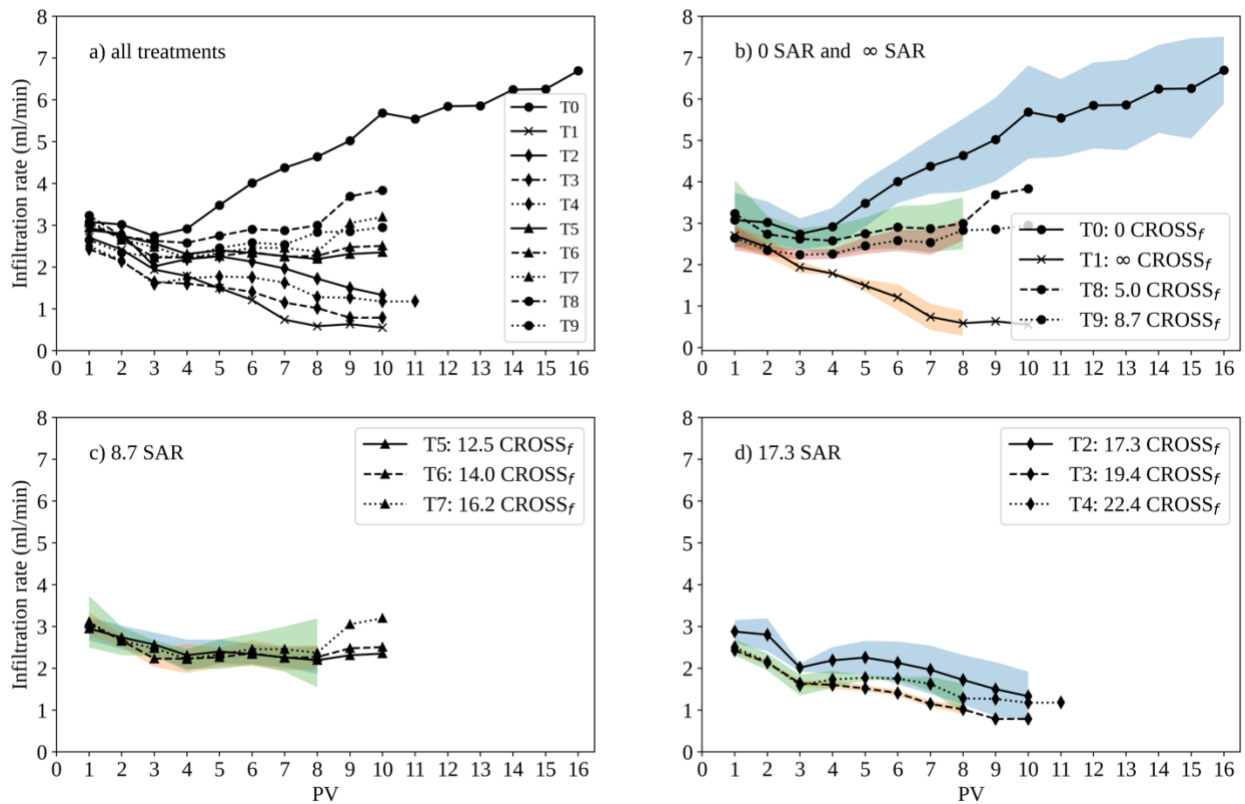


Figure 2.3: Saturated hydraulic conductivity (ml/min) over the pore volume application of the recycled water cation treatments where: a) average infiltration rate for all treatments; b) 0-SAR and infinity SAR treatments; c) 8.7-SAR treatments; d) 17.3-SAR treatments. The shaded area represented the standard error.

Table 2.3: Statistical analysis of the log-transformed saturated infiltration rate. Similar letters indicate no statistical difference at  $P < 0.05$ . The treatments are arranged in descending order of the overall average infiltration rate.

Treatment	
T0	A
T8	B
T9	B C
T7	B C
T5	B C
T6	B C
T2	C D
T4	D E
T3	D E
T1	E

The saturated infiltration rate was further analyzed concerning the different cation ratios. The correlation was tested at pore volume 8 (Figure 2.4). Pore volume 8 was chosen to ensure ample time for the cation exchange and to guarantee a minimum of three measurements per treatment. The observed general trend is that the infiltration rate decreases with increasing cation ratios.  $CROSS_f$  demonstrated a stronger correlation with an  $R^2$  of 0.90. Conversely,  $CROSS_{opt}$  exhibited the least correlation with an  $R^2$  of 0.41 which could indicate that  $CROSS_{opt}$  had a good correlation with the TEC under the specific study conditions outlined in Smith et al. (2015) but may not be generalizable.

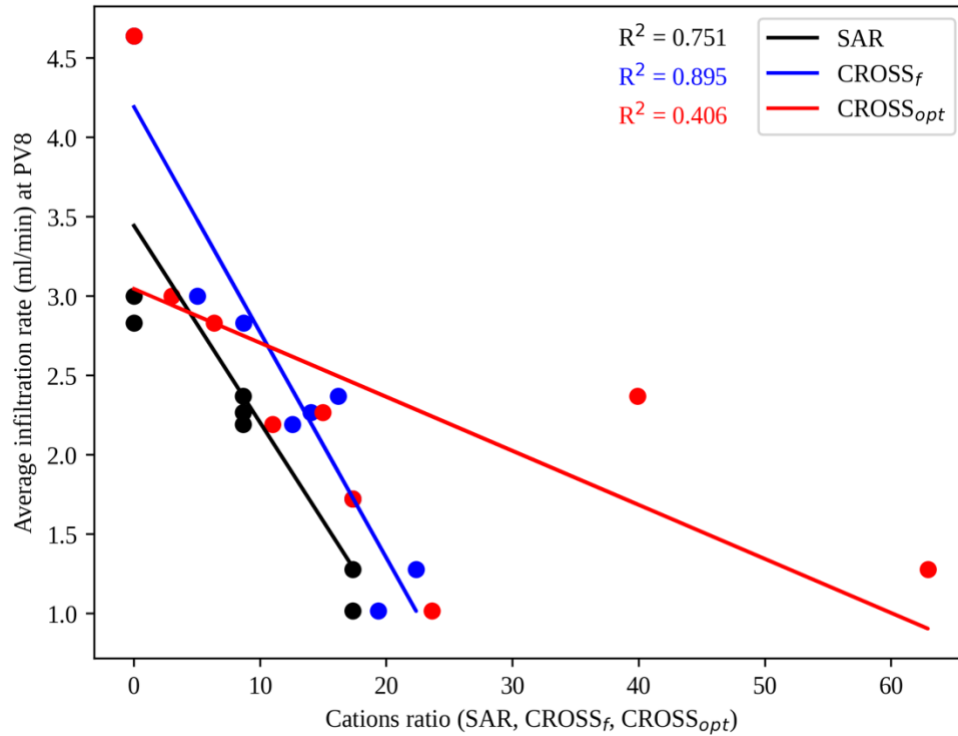


Figure 2.4: The correlation of the average infiltration rate at the eighth pore volume (PV8) with the cation ratios (SAR, CROSS<sub>f</sub> and CROSS<sub>opt</sub>).

The drainage rate from the columns was analyzed. The drainage rate was plotted versus the infiltration rate (Figure 2.5). The correlation yielded a 1:1 line indicative of a balanced correspondence between the amount infiltrated and the subsequent drainage with an RMSE of 0.02. The result further proves that saturated hydraulic conductivity can be determined from the drainage rate if the water head above the soil surface is greater than zero.

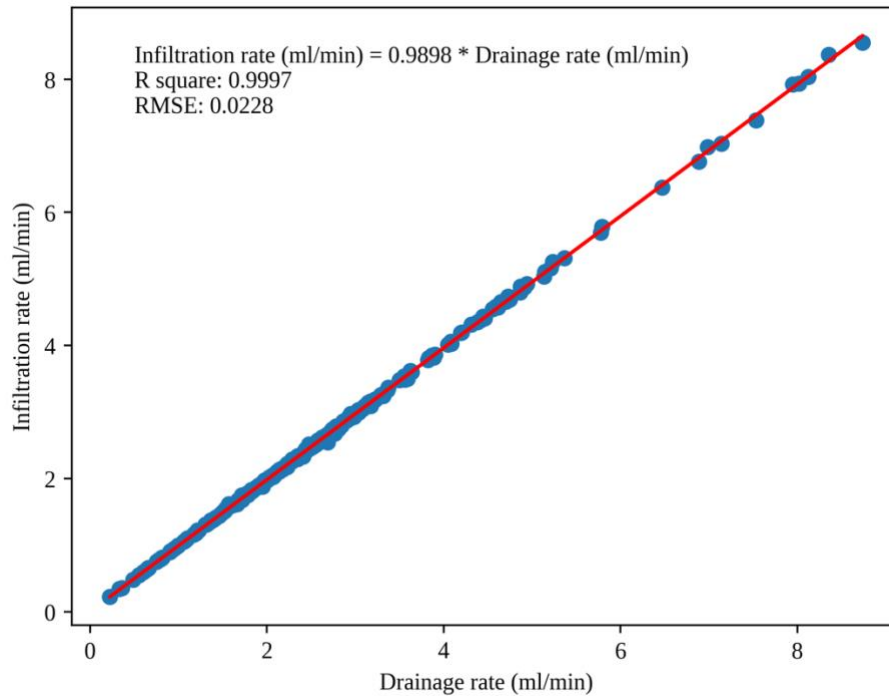


Figure 2.5: Correlation of the drainage rate from the soil column and the subsequent infiltration rate indicating that input equals output.

### 2.3.3. Soil structure evaluation:

The condition of the soil surface within the soil column was observed through photographs taken before and after conducting the infiltration experiment. Table 2.4 illustrates the conditions of the soil surface for the calcium chloride treatment (T0) and the sodium chloride treatment (T1) before and after the experiment. The aggregates of the soil particles hardly changed after applying the calcium chloride solution for 16 pore volumes of the solution. However, the soil surface condition of T1 was completely dispersed with all aggregates breaking down after the application of only 8 pore volumes of the solution. Certainly, the calcium cations in T0 helped maintain the soil structure's condition. Conversely, the sodium cations caused

aggregate dispersion into individual soil particles reducing the number of macropores and leading to soil surface clogging.

Table 2.4: Photographs showing the top surface of the soil within the soil column for treatments T0 (calcium chloride) and T1 (sodium chloride) before and after conducting the infiltration experiment.

T	Before applying the treatment	After applying the treatment
T0		
T1		

Figure 2.6 shows the relative clay percentage between treatments T0 and T1 as a function of agitation and circulation time and circulation time. There was no statistical significance between Figure 2.6a (agitation and circulation) and Figure 2.6b (circulation) which could indicate that agitation had no effect. Both methods showed increasing clay percent detection over time for both T1 and T0. T1 consistently exhibited higher values compared to T0, as T1 contained sodium chloride in its solution resulting in soil with lower aggregate stability. In contrast, the use of calcium chloride in T0 led to improved aggregate stability. The results from Tukey-Kramer's HSD test indicated a statistically significant difference.

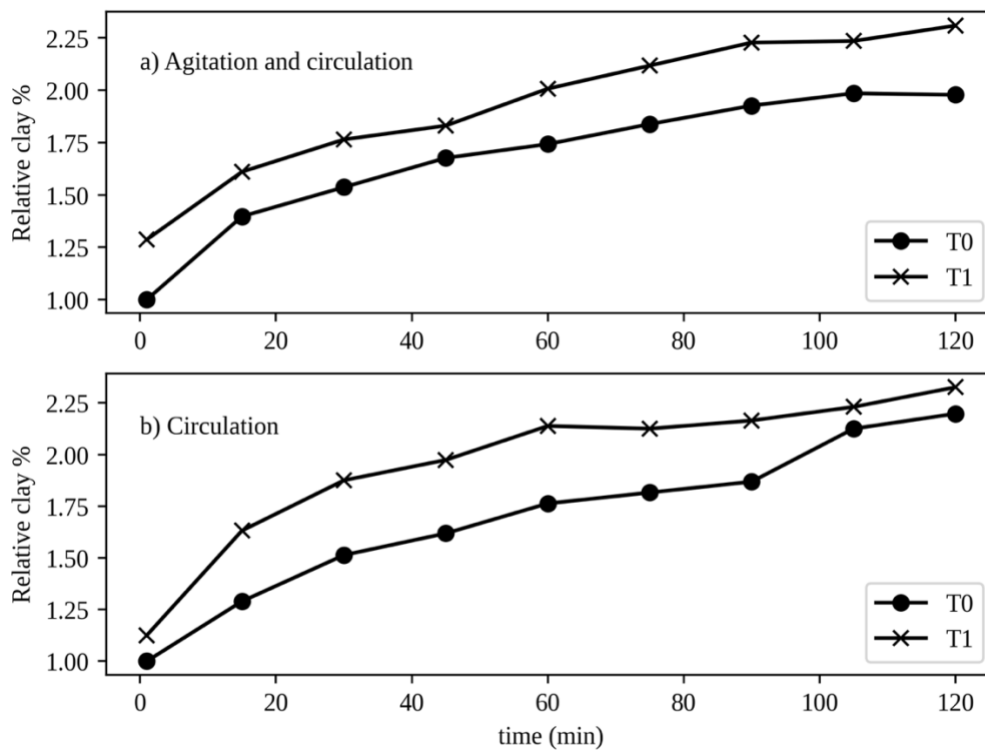


Figure 2.6: Clay dispersion over time evaluated using a Laser Scattering Particle Size Distribution Analyzer (Partica LA-960V2, HORIBA, Ltd.) for the top 1 cm sample collected from the soil column at the end of the experiment.

Due to the minor distinction between the two extreme conditions (T0 and T1), assessing the stability of the remaining treatments using the Particle Size Distribution Analyzer was challenging. This was attributed to the requirement of a very small sample (0.1 to 0.5 g) for accurate particle characterization by the Particle Size Distribution Analyzer. The small sample size, in comparison to the additional deionized water introduced by the instrument, led to sample dispersion due to the presence of the deionized water.

To compare all the treatments, soil structure was evaluated using the spontaneous dispersible clay method. The results of the clay dispersion analyses are presented in Figure 2.7, with each curve encircled by a shaded area indicating the associated standard error. Subsequently, the output of Tukey-Kramer's HSD test is outlined in Table 2.5. Clearly, treatment T0 (calcium chloride solution) was statistically more significant than the rest of the treatments. The treatment solution helped to improve the soil structure along the entire column length. Although, treatments T8 and T9 had a 0-SAR like T0, they were statistically more significant than T0 for the entire soil column. This indicates that the observed clay dispersion was due to the potassium content in the treatment solutions.

The highest average observed clay dispersion was for treatment T1 and it was not statistically significant compared to treatments T2, T3 and T4 (17.3-SAR). Similarly, there was no statistical significance among the 8.7-SAR and 0-SAR (T8 and T9). This could be due to the fact that the clay dispersion is generally reduced by depth (like T1). Tukey-Kramer's HSD test was further used to compare the effect of the depth of the sample. The clay dispersion at 1 cm was found to be statistically more significant than at depths of 5 cm, 25 cm and 45 cm. The samples collected from 5 cm, 25 cm and 45 cm depths were not statistically significant. This

could imply that most of the clay dispersion happens at the surface, making the infiltration issue more closely related to the state of the uppermost layer.

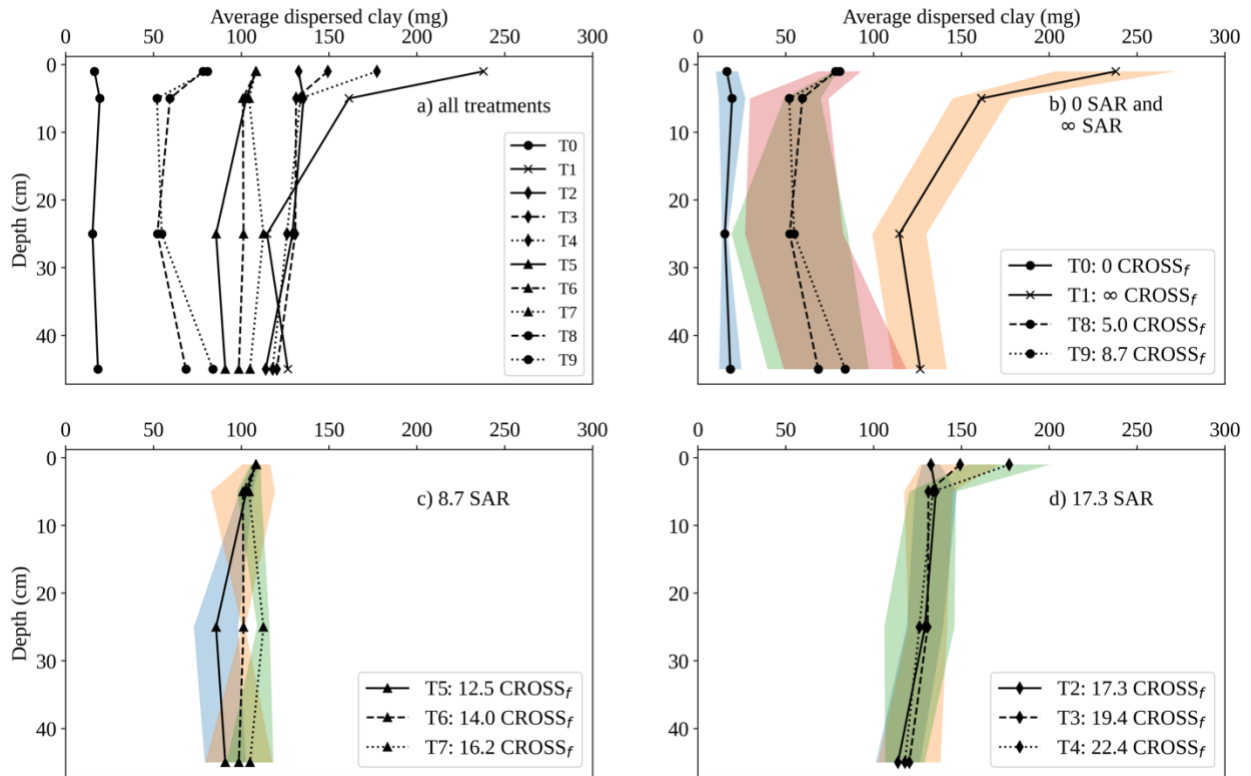


Figure 2.7: Average clay dispersion of the samples collected from soil column by depth at the end of the infiltration experiment where: a) all treatment; b) 0-SAR and infinity SAR treatments; c) 8.7-SAR treatments; d) 17.3-SAR treatments. The shaded area represented the standard error.

Table 2.5: Statistical analysis of the clay dispersion for the entire soil column. Similar letters indicate no statistical difference. The treatments are arranged in descending order of the overall average dispersible clay at  $P < 0.05$ .

Treatment	
T1	A
T4	A B
T3	A B C
T2	A B C
T7	B C
T6	B C D
T5	C D
T9	D
T8	D
T0	E

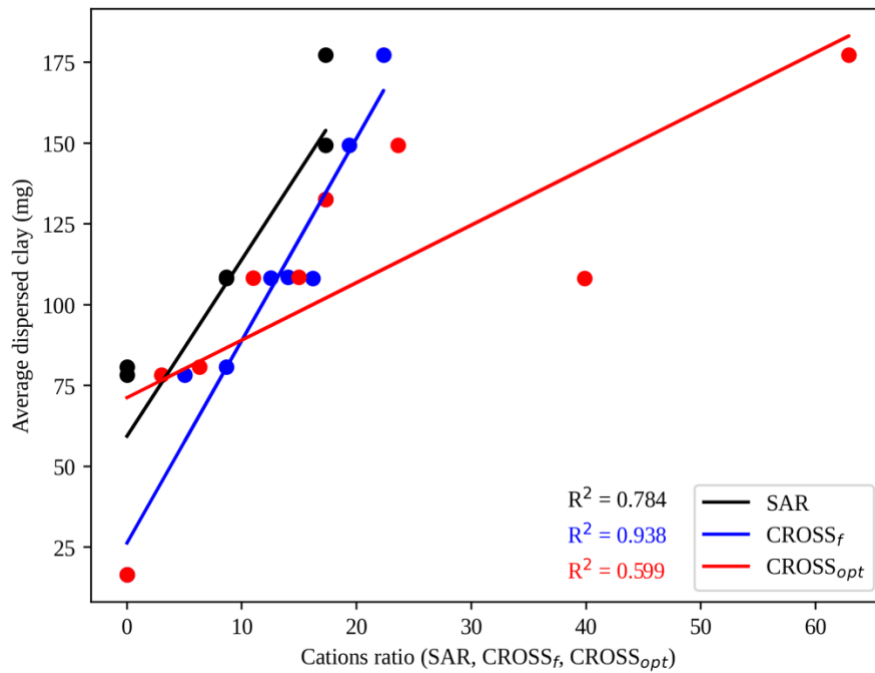


Figure 2.8: Correlation of the average spontaneous clay dispersion for the top 1 cm samples collected from the soil columns at the end of the infiltration experiment.

Therefore, the correlation test with cation ratios for average clay dispersion was evaluated for the clay dispersion measured from the 1 cm samples (Figure 2.8). Generally, the clay dispersion increased with increasing cation ratios.  $CROSS_f$  had better correlation with  $R^2$  of 0.94 and the least correlation was observed for the  $CROSS_{opt}$  with  $R^2$  of 0.60.

#### 2.4. Conclusions:

A soil column experiment was conducted to evaluate the combined effect of the sodium, potassium, calcium and/or magnesium cations in recycle water on soil infiltration and soil structure. Those solutions were synthetically made to mimic low quality waters like recycled water as recycled waters usually have low salinity levels but most of the time their monovalent cation presence is higher than their divalent cation presence. A Wooding infiltrometer was used to evaluate impacts on the saturated hydraulic conductivity ( $K_{sat}$ ).

Initially, the sensors attached to the infiltrometer and connected to the datalogger were calibrated. After conducting the infiltration experiment, the sensors were tested for their performance by comparing the 1:1 line of sensor output  $K_{sat}$  with the observed  $K_{sat}$  and evaluating the root mean square error (RMSE). The result showed strong agreement with a unit  $R^2$  and zero RMSE. The drainage rate was compared with the infiltration rate and found to be equal to the saturated infiltration rate. The  $K_{sat}$  was then evaluated over the pore volume. The analyses of the infiltration rate showed a strong correlation with the cation ratio of soil structure stability ( $CROSS_f$ ) with a  $R^2$  of 0.90 as compared with SAR's  $R^2$  of 0.75.

The soil structure was evaluated by a Laser Scattering Particle Size Distribution Analyzer. Since the sample size of the analysis was too small, it was very difficult to find a protocol to assess the clay dispersion for various values of SAR or CROSS. However, the

calcium chloride treatment (T0) and sodium chloride treatment (T1) were analyzed for the samples collected from the top 1 cm. Treatment T1 resulted in a statistically significant higher clay percent detection than treatment T0. Clay dispersion was evaluated at different depths. Overall, there was a slight reduction in the clay dispersion with increasing depth indicating that most of the clay dispersion occurred at the surface and that the clay dispersion of the top 1 cm was statistically more significant than the lower depths. The correlation of the average clay dispersion of the top 1 cm sample showed a strong correlation with  $CROSS_f$  with an  $R^2$  of 0.94 as compared with SAR's  $R^2$  of 0.78.

The outcome of the study experimentally confirmed that potassium contributed significantly to the possible changes in the soil's physical properties and magnesium had less flocculating power than calcium. For future work, it is recommended that treatments be designed such that the values of  $CROSS_f$  have more spread at a given SAR. This could improve the statistical analysis.

## Chapter 3

### Assessing the impact of recycled water reuse for irrigation on soil hydrology in a greenhouse

#### 3.1. Introduction:

Freshwater scarcity, coupled with the increasing world population, is a major driving force behind recycled water reuse. Globally, about 2.3 billion people lack access to safe drinking water, according to WHO (2022). A significant portion of freshwater is allocated to the agricultural sector. Globally, the agricultural sector accounts for the largest share of freshwater usage, with 70 percent of the total freshwater (Gleick and Heberger, 2014). Recycled water reuse for irrigation purposes can serve as an alternative water supply to sustain agricultural production for the growing population. This practice can also help meet both environmental functional flows and domestic water demands using freshwater. Furthermore, recycled water reuse for irrigation can assist in overcoming groundwater overdraft by reducing the amount of freshwater that agriculture withdraws.

Recycled water use in agriculture has its challenges. When using primary or secondary treated wastewater, soil salinity buildup could be significant within a few years of application due to high dissolved salts. For example, soil salinity increased by 123% after only three years of irrigation with secondary treated wastewater in Glen Valley, Australia (Dikinya and Areola, 2010). In some southern California recreational fields, irrigating with potable water has replaced the use of recycled water due to its high total dissolved solids (LaSalle, 2018). Other studies have also reported increases in salinity when using primary or secondary treated wastewater (Jahantigh, 2008; Klay et al., 2010; Xu et al., 2010).

Tertiary or advanced treated wastewaters, on the other hand, have even lower salinity levels than freshwater. However, they differ from freshwater in terms of the presence of constituents with different ratios. For example, the availability of potassium in natural water and in soils irrigated with it is minimal (Richards, 1954) but its occurrence in treated wastewater is considerable and varies depending on the source of the wastewater (Arienzo et al., 2009; Chand et al., 2020). Additionally, potassium can present in the soil due manure fertilizer from animals fed with potassium-rich diet like alfalfa (Wallender and Tanji, 1990). Consequently, the application of recycled water has a greater impact on soil sodicity than freshwater due to the elevated concentration of certain constituents such as sodium and potassium (Sposito et al., 2016).

The commonly used method to assess soil infiltration based on irrigation water quality is the Sodium Adsorption Ratio (SAR), which considers sodium as the primary cation responsible for alkali hazard (Richards, 1954). However, SAR ignores potassium's effect as a dispersive agent and the influence of each cation on clay dispersion or flocculation. Potassium has affirmative impacts on soil permeability (Ahmed et al., 1969; Arienzo et al., 2009; Chen et al., 1983; Gardner et al., 1959; Martin and Richards, 1959; Quirk and Schofield, 1955; Reeve et al., 1954; Rengasamy and Marchuk, 2011; Smith et al., 2015). Based on Chen et al. (1983), some studies, however, reported that soil aggregates exhibited better stability in potassium-saturated soils compared to calcium- or magnesium-saturated soils (Cecconi et al., 1963; Ravina, 1973).

Rengasamy and Marchuk (2011) developed the Cation Ratio of Soil Structural Stability (CROSS) relation to account for potassium effect as well as the relative flocculating power of the cations (sodium, potassium, calcium and magnesium). The CROSS relation was found to have a better predictability of soil aggregate dispersion compared to the SAR relation. Therefore, the

CROSS relation could be a more suitable sodicity standard for waters of marginal quality. However, relations other than SAR remains understudied with respect to infiltration rate, permeability and water holding capacity. To address this gap, the present study aimed to investigate the interaction between monovalent cations (sodium and potassium) and divalent cations (calcium and magnesium) on soil infiltration rate, soil water storage, permeability and soil structure. To achieve this objective, synthetic recycled water of varying quality was prepared by adjusting the concentrations of the cations. The prepared synthetic water was then used to irrigate clay loam soils in pots and strawberry plants in the greenhouse.

### 3.2. Methodology:

#### 3.2.1. Experimental set up:

Soil was collected from an agricultural research field at the University of California Davis, near Davis CA. The soil was taken from the top 0 to 30 cm soil surface after removing the small layer at the top (5 to 10 cm) that could potentially contain a high level of organic matter. Table 3.1 lists the properties of the collected soil.

Pots were filled with the air-dried soil that was screened through a 6 mm sieve to provide a reasonable starting point for soil structure comparable to field conditions. Three successive layers were packed carefully to achieve an average bulk density of  $1.3 \text{ g/cm}^3$  which was similar to that measured in the field. The top of each layer was shattered to minimize layer-to-layer stratification. The total water content was accounted for by measuring the moisture content of the air-dried soil which was  $59.5 \text{ mg-water/g-soil}$  ( $\pm 5.0$ ,  $n=15$ ). A total of 176 pots were prepared with four replicates per treatment and four pots per replication. The experiment followed a complete randomized block design with four blocks and 11 treatments.

Table 3.1: Properties of the soil used in the experiment and the method of determination.

Parameter (unit)	Average value (standard deviation)	Method/tool
EC <sub>e</sub> (dS/m)	0.95 (±0.06)	Saturated paste extract
pH	7.1 (±0.53)	Saturated paste extract
sand (%)	35.06 (±0.86)	Hydrometer method
silt (%)	31.56 (±1.73)	Hydrometer method
clay (%)	33.38% (±1.25)	Hydrometer method
gravel (%)	0.06% (±0.06)	Gravimetric (scale)
texture	clay loam	Soil texture triangle
field BD (g/cm <sup>3</sup> )	1.33 (±0.09)	Core sample
organic carbon	1.26 (±0.08)	Loss-on-ignition
Exchangeable Na (meq/100g)	0.13 (±0.01)	ICP-AES
Exchangeable K (meq/100g)	0.83 (±0.07)	ICP-AES
Exchangeable Ca (meq/100g)	8.27 (±0.25)	ICP-AES
Exchangeable Mg (meq/100g)	11.83 (±0.32)	ICP-AES
CEC (meq/100g)	21.1 (±0.53)	Measured
ESP (%)	0.60 (±0.53)	Measured
dominant clay mineral	Montmorillonite	From literature <sup>1</sup>

<sup>1</sup> From Dasberg and Hopmans (1992) and Lagerwerff and Brower (1972)

The treatments were designed to mimic treated wastewater with specific cationic content to evaluate the parameters used to predict infiltration and soil structure degradation. All treatments had an electrical conductivity of 1.5 dS/m using chloride solutions of sodium, potassium, calcium and/or magnesium except for one treatment made of calcium sulfate (Table 3.2) which was used to evaluate the effect of chloride on the plants (Aldughaiishi et al., 2024). The treatments were designed to have SAR values of 0, 4.9, 9.8 and infinity (sodium chloride solution). The same treatments had CROSS<sub>f</sub> and CROSS<sub>opt</sub> values ranging from 0 to 12.6 and from 0 to 35.6, respectively.

The treatments were applied to the soil in the pots using drip irrigation which was based on two criteria: leaching factor of 30% to maintain the soil EC below the threshold EC<sub>e</sub> of strawberry plants and a tensiometer reading below 10 kPa (Figure 3.1). The soil in the pots was irrigated every day throughout the 40-weeks growing period. From the start of the irrigation (week 1) to week 22, the irrigation was provided in 50 ml pulses every 15 mins. After week 22,

the irrigation was provided in 100 ml pulses every 15 mins. The irrigation was provided between the hours of 11:00 AM to 1:15 PM.

Table 3.2: Synthetic recycled water chemical composition for various treatments.

Treatments	T0	T1	T2	T3	T4	T5	T6	T7	T8	T9	T10
EC (dS/m)	1.5	1.5	1.5	1.5	1.5	1.5	1.5	1.5	1.5	1.5	1.5
NaCl (mmol/L)	0	15	12	12	12	6	6	6	0	0	0
KCl (mmol/L)	0	0	0	0	0	6	6	6	12	12	12
CaCl <sub>2</sub> (mmol/L)	0	0	1.5	0.75	0	1.5	0.75	0	1.5	0.75	0
MgCl <sub>2</sub> (mmol/L)	0	0	0	0.75	1.5	0	0.75	1.5	0	0.75	1.5
CaSO <sub>4</sub> (mmol/L)	20	0	0	0	0	0	0	0	0	0	0
SAR	0	∞	9.80	9.80	9.80	4.90	4.90	4.90	0	0	0
CROSS <sub>f</sub>	0	∞	9.80	10.95	12.65	7.64	8.54	9.87	5.49	6.13	7.08
CROSS <sub>opt</sub>	0	∞	9.80	13.36	35.59	6.54	8.92	23.75	3.28	4.48	11.92

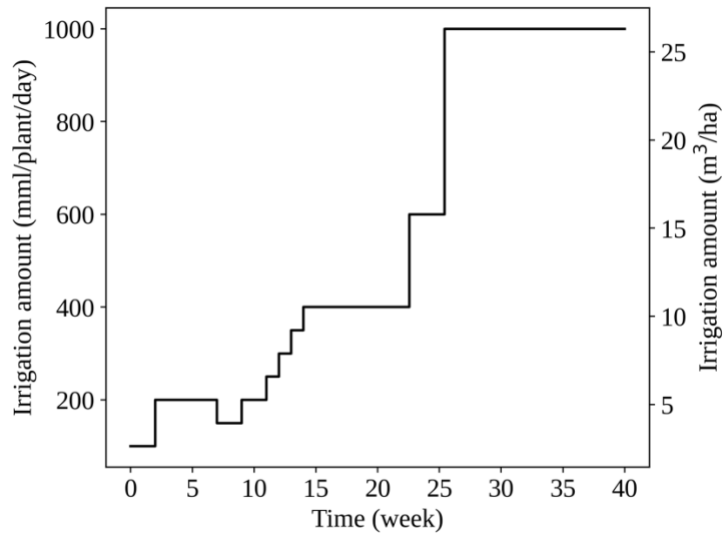


Figure 3.1: Irrigation scheduling based on leaching factor and the tensiometer readings.

### 3.2.2. Soil permeability evaluation:

The impact of recycled water reuse on soil structure was evaluated by counting the number of pots with standing water, which indicates poor infiltration and soil structure degradation. Two permeability tests were performed. The first test was conducted every two weeks during the growing period from week 26 to week 38 by counting the number of pots with standing water about an hour before the next irrigation event. The second test was performed at the end of the experiment over a period of 39 hours, starting from time 0 (exactly when irrigation stopped). The measurements were taken while the plants were still in the pots and with varying frequencies: 0, 0.5, 1, 1.5, 2, 3, 6, 15, 27 and 39 hours. The results were reported as the percentage of pots with standing water.

### 3.2.3. Relative hydraulic conductivity:

To determine the impact of the treatments used in the irrigation on soil hydraulic conductivity, we conducted infiltration tests on three randomly selected pots from each of the 11 treatments at the end of the greenhouse experiments after removing the shoots of the plants (the roots were not removed from the soil). The wooding infiltrometer was used and a total of 33 infiltration tests were conducted. Infiltration rates were then correlated with SAR,  $CROSS_f$  and  $CROSS_{opt}$ . The results of the wooding infiltrometer were reported as relative hydraulic conductivity relative to treatment 0 because the actual saturated hydraulic conductivity could not be measured for several reasons. First, the size of the pots was larger than the size of the infiltrometer base, so a soil ring was used above the soil in the pots. Second, it was required to measure the moisture content before running the infiltration test and after the infiltration test. The later can be performed with no issue, however, the former was not possible without

damaging the soil and causing channels through the pots. Third, the pots were not wide enough to ensure consistent lateral water movement like in the field. Lastly, the pots had a larger top diameter than the bottom. Therefore, each infiltration test was run for about an hour for each replication and the last few datapoints (around 8) were used to estimate the infiltration rate from the slope of the line of the cumulative infiltrated water depth over time. The measured infiltration rate of treatment 0 was used as a reference point to the other treatments.

#### 3.2.4. Soil moisture evaluation:

Soil moisture content was measured 4 and 7 days after the end of the experiment (after removing the plants) without irrigation. Analysis of the water holding capacity was conducted using a TDR sensor (Acclima Inc, Meridian Idaho). The 4-day measurement was found to be insignificant among the treatments and therefore only the analysis of the 7-day moisture content was considered in the analyses. Thirteen measurement per treatment were taken from all pots except those used for the infiltration experiment.

#### 3.2.5. Soil structure evaluation by clay dispersion:

Samples were collected from the pots 5 to 10 cm and 10 to 15 cm depth with four replicates from each treatment (a total of 88 samples) using a soil auger sampler. The top layer of soil (0 to 5 cm) was excluded from the analysis due to high fertilizer levels. The estimation of dispersed clay followed the method of spontaneous dispersion developed by Marchuk et al. (2013). For this analysis, 40 g of an oven-dried sample collected from the pots were placed in 250 ml graduated cylinder and 200 ml of deionized water was added. The mixture was left for 5 hours and then the soil was stirred into suspensions and left to stand for 2 hours. To estimate the

dispersed clay, 10 ml of the solution was pipetted from a depth of 10 cm and the solution was oven-dried to obtain the weight (mg) using a sensitive scale with an accuracy of  $\pm 0.1$  mg.

### 3.2.6. Models for predicting soil permeability hazards from using water of marginal quality:

The common soil infiltration assessment based on irrigation water quality is the Sodium Adsorption Ratio (SAR) (Richards, 1954):

$$SAR = \frac{Na^+}{\sqrt{Ca^{2+} + Mg^{2+}}} \quad 3.1$$

where  $Na^+$ ,  $Ca^{2+}$  and  $Mg^{2+}$  are the concentrations of the ions in mmol/L. Regarding monovalent and divalent cation weight on clay dispersion or flocculation, Rengasamy and Marchuk (2011) developed the Cation Ratio of Soil Structural Stability (CROSS):

$$CROSS_f = \frac{Na^+ + 0.56 * K^+}{\sqrt{Ca^{2+} + 0.60 * Mg^{2+}}} \quad 3.2$$

where  $K^+$  is the concentration of the potassium ion in mmol/L. The subscript  $f$  indicates that the factors of K and Mg “are based on the relative flocculating power”. Equation 2 has better soil infiltration predictability (based on the dispersion of aggregates) than SAR. Smith et al. (2015) further optimized equation 2 to provide best-fit factors less than one for K and Mg using threshold electrolyte concentration (TEC) experimental data from Arienzo et al. (2012). The result was:

$$CROSS_{opt} = \frac{Na^+ + 0.335 * K^+}{\sqrt{Ca^{2+} + 0.0758 * Mg^{2+}}} \quad 3.3$$

where the subscript  $opt$  indicates optimization.  $CROSS_{opt}$  has a better predictivity of TEC than SAR and  $CROSS_f$ .

### 3.2.7. Statistical analysis:

A one-way analysis of variance (ANOVA) was used to determine if the treatments within the groups differed statistically, using a significance level ( $\alpha$ ) of 0.05. The Python library 'scipy.stats' and 'f\_oneway' function was used to execute the ANOVA test. This function allowed for the calculation of the F-statistic and corresponding p-value, which were used to evaluate treatment group mean differences.

## 3.3. Results and Discussion:

### 3.3.1. Soil permeability evaluation:

Figure 3.2 shows the results of the permeability test conducted during the growing period. Figure 3.2a shows the outcomes of all treatments which were statistically significant ( $P < 0.05$  and  $F\text{-stat} = 25.17$ ). The results reveal that T0 (gypsum solution) had the lowest number of pots with standing water followed by the zero-SAR treatments (T8, T9 and T10). Conversely, T1 (sodium chloride solution) had the highest number of pots with standing water with over 80% after week 28. This indicates that the soil was becoming clogged and impeding water drainage, which was also observed in some other treatments such as T2, T3, T4, T6 and T7, where pots with standing water exceeded 30%.

Figure 3.2b compares the 0-SAR treatments ( $P < 0.05$  and  $F\text{-stat} = 3.94$ ) with the sodium chloride treatment. T0 exhibited less clogging over the measured period, indicating that T8, T9, T10 (0-SAR) are different than T0. Figure 3.2c and d compare treatments that had 4.9-SAR ( $P < 0.05$  and  $F\text{-stat} = 12.17$ ) and 9.8-SAR ( $P < 0.05$  and  $F\text{-stat} = 6.01$ ), respectively. The distinction between the treatments of 4.9-SAR is in line with the  $CROSS_f$  value, indicating that as  $CROSS_f$  increases, the soil's drainage capacity decreases.

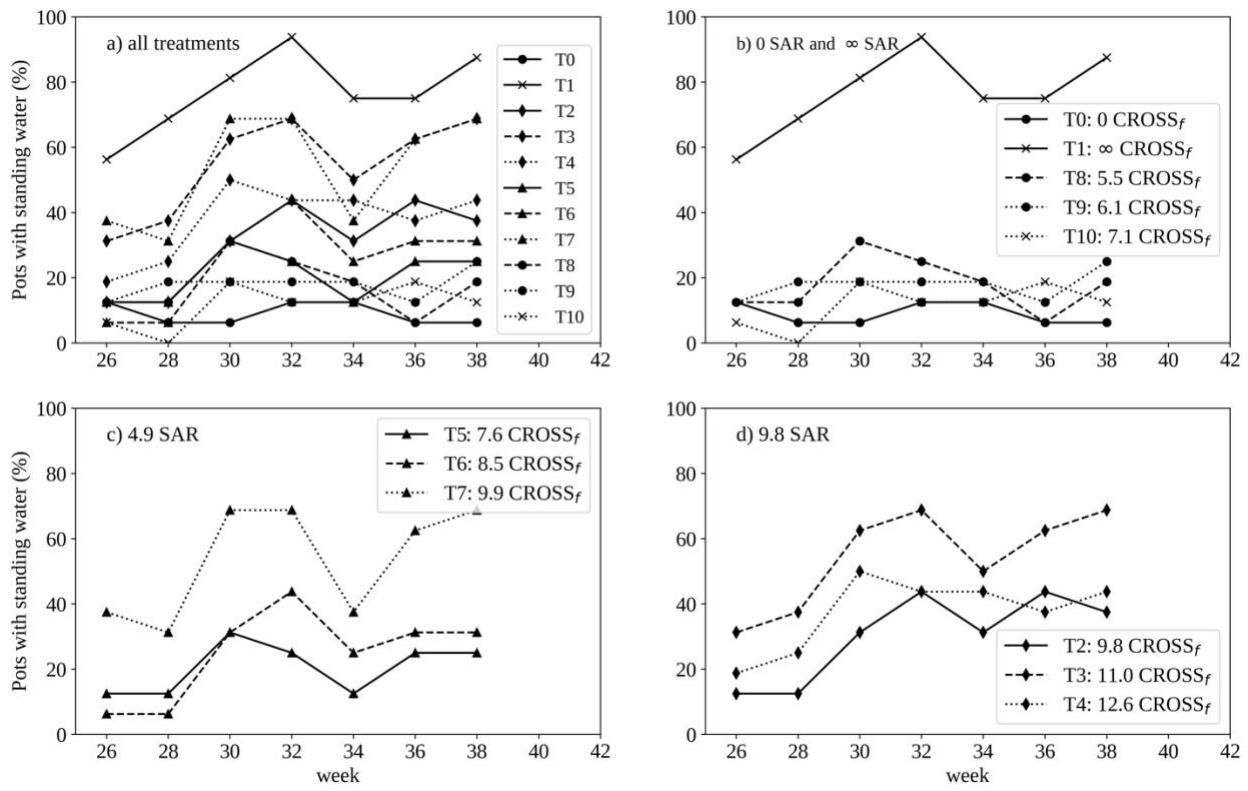


Figure 3.2: Permeability test measured as percent of pots with standing water over the growing period from week 26 to 38; a) all treatments, b) 0-SAR and  $\infty$  SAR, c) 4.9-SAR and d) 9.8-SAR.

The correlation results presented in Figure 3.2 could not be evaluated because the measurement was taken one hour before the subsequent irrigation event. This implies that the measurement was obtained about 20 hours after the end of the previous irrigation. The analysis of the permeability over time (Table 3.3) revealed that the correlation was more significant within the first six hours. Afterward, the trend could not be established as more pots were drained due to cut of irrigation and evaporation.

Figure 3.3 depicts the permeability test results at the end of the experiment. The number of pots with standing water was recorded over a period of 39 hours. Figure 3.3a provides an

analysis of all treatments indicating that T1 had a higher number of pots with standing water compared to other treatments. Figure 3.3b compares the treatments with 0-SAR, showing that T0 had a relatively minor impact in comparison to the other treatments. Figure 3.3c and 3.3d compare treatments with 4.9-SAR and 9.8-SAR, respectively. Furthermore, a correlation test was conducted at a specific time to examine the relationship between permeability and SAR,  $CROSS_f$  and optimized CROSS.

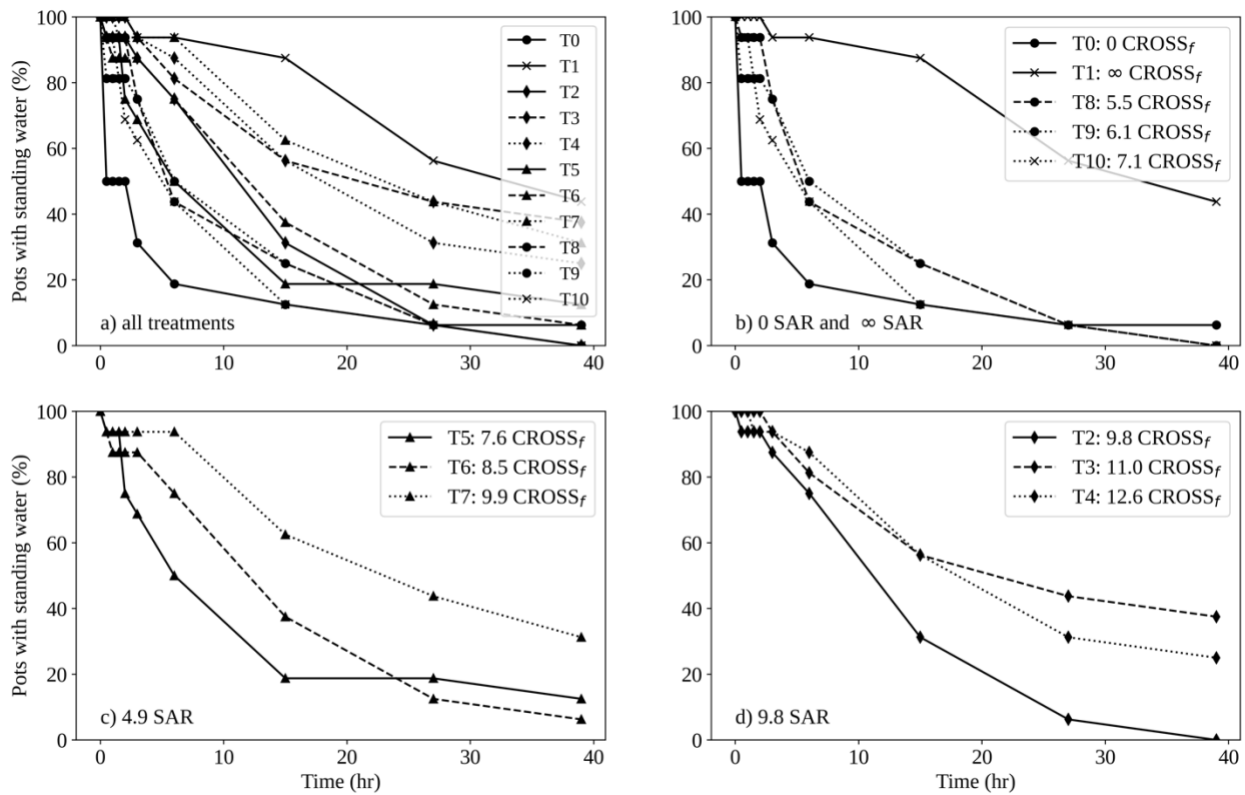


Figure 3.3: Percentage of pots with standing water after the end of the last irrigation for a) all treatments, b) 0-SAR and  $\infty$  SAR, c) 4.9-SAR and d) 9.8-SAR.

Figure 3.4 illustrates the correlation between the data collected 6 hours after cutting off irrigation. The results indicate that an increase in cation ratios leads to a decrease in the ability to

drain water. Nonetheless, the permeability issue is more closely correlated with  $CROSS_f$ , having an R squared of 0.84, as opposed to SAR and optimized CROSS which have R squared values of 0.63 and 0.59, respectively. The correlation results within the 6-hours timeframe (Table 3.3) exhibit the same trend, suggesting that the decrease in drainage is more closely associated with  $CROSS_f$ . Notably, the correlations results excluded T1 which has an infinite value of the cation ratio. However, T1 exhibited the highest number of pots with standing water over the 39-hours period.

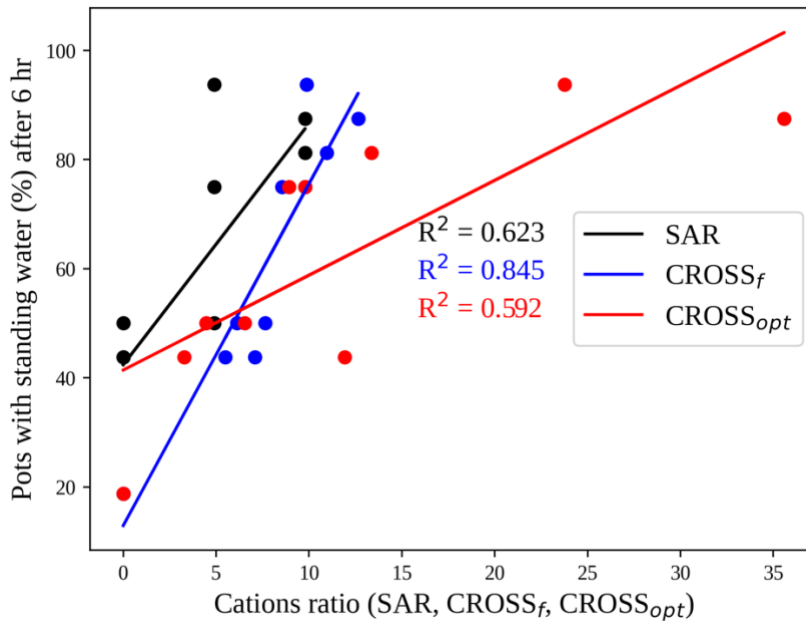


Figure 3.4: Correlation between pots with standing water after 6 hr and the cations ratio (SAR,  $CROSS_f$ ,  $CROSS_{opt}$ ).

Table 3.3: Coefficient of determinations ( $R^2$ ) of the regression line correlations of pots with standing water (%) and cations ratio.

Time (hr)	SAR	CROSS <sub>f</sub>	CROSS <sub>opt</sub>
0.5	0.31	0.78	0.29
1	0.30	0.77	0.31
1.5	0.37	0.73	0.21
2	0.41	0.67	0.24
3	0.49	0.86	0.40
6	0.62	0.84	0.59
15	0.48	0.59	0.59
27	0.36	0.40	0.46
39	0.37	0.32	0.41

### 3.3.2. Relative hydraulic conductivity:

Figure 3.5 displays the correlations between cation ratios (SAR, CROSS<sub>f</sub>, CROSS<sub>opt</sub>) and the relative average infiltration rates measured using a Wooding Infiltrometer in soil pots.

Generally, the results indicate that an increase in cation ratios leads to a decrease in the relative infiltration rate. The 0-SAR group (T0, T8, T9 and T10) and the 9.8-SAR group (T2, T3 and T4) are statistically significant with  $P < 0.05$ , with F-statistics of 5.4 and 42.29, respectively.

However, the 4.9-SAR group was not statistically significant. The average infiltration rate was highly correlated with CROSS<sub>f</sub> (R squared value of 0.6) followed by CROSS<sub>opt</sub> (R squared value of 0.4) and least correlated with SAR (R squared value of 0.2). T1, which used sodium chloride solution (not shown in the graphs), had the lowest infiltration rate with an average relative infiltration rate of 0.068 and a standard deviation of  $\pm 0.010$ . The infiltration rate of T1 was 93% lower than that of gypsum treatment (T0) and 47% lower than T4 (the treatment with the second lowest relative infiltration rate). These findings provide evidence that CROSS<sub>f</sub> is a better



9.8, resulting in a similar effect soil moisture storage. Typically, poorly drained soils retain more water for longer periods than well-drained structured soils. The correlation results in Figure 3.6b indicate a higher correlation between  $CROSS_f$  and soil moisture (R squared value of 0.6) compared to SAR and soil moisture (R squared value of 0.4) and  $CROSS_{opt}$  (R squared value 0.31).

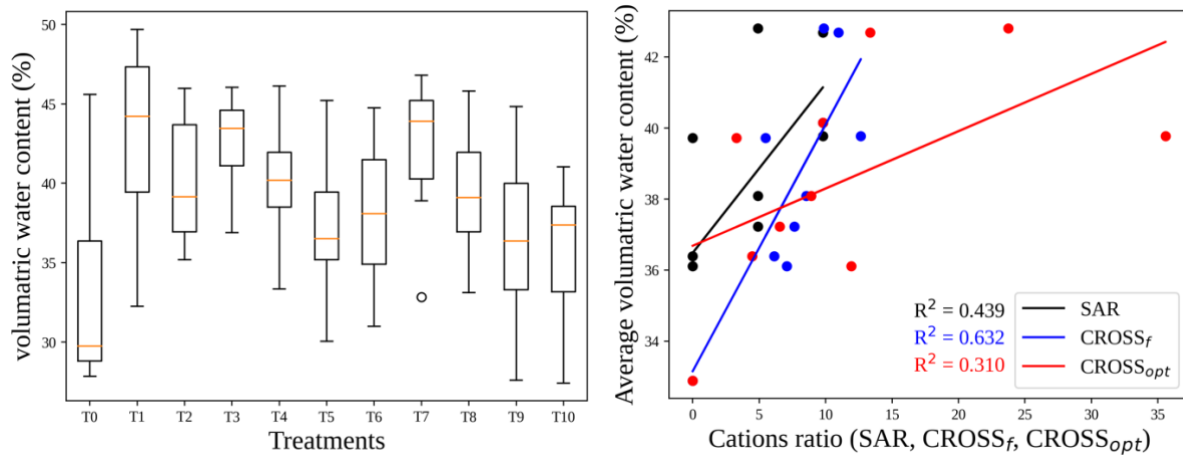


Figure 3.6. a) Box plot of the volumetric moisture Content measured in pots after 7 days from terminating the irrigation (n=13) in synthetic recycled water treatments. b) Correlation between the average volumetric water content and cation ratios (SAR,  $CROSS_f$ ,  $CROSS_{opt}$ )

The main factors that affect the water holding capacity of soil are its texture and structure. Therefore, the increase in the average volumetric soil water content due to the application of the treatments is mainly caused by the change in the soil structure rather than an actual increase in available water for the plants. This measurement could mislead farmers into thinking that the soil has sufficient moisture for their plants in real practice. In reality, the high moisture content may be due to the soil structure degradation. This was also observed by Farahani et al. (2020) who concluded that the having higher moisture available for the plants is

beneficial. However, in the long run, the application of recycled water under these conditions is not sustainable.

#### 3.3.4. Dispersed clay:

A statistical difference in clay dispersion was not found between the depths of 5 to 10 cm and 10 to 15 cm in block 1. Consequently, for the remaining replicates in block 2, 3 and 4, the samples were combined. The results displayed in Figure 3.7 depict samples gathered from a depth of 5 to 15 cm. Each data point indicates the mean of dispersed clay from four samples (one sample per block) and each sample per replication was a combination of soil from 2-4 pots collected from a depth of 5 to 15 cm. The error bars represent the standard deviation around the mean. Only the 0-SAR group was found to be statistically significant ( $P < 0.05$ ,  $F\text{-stat} = 11.25$ ). The average dispersed clay had a strong correlation with  $CROSS_f$  with an R squared of 0.97, compared to SAR and  $CROSS_{opt}$  with R squared of 0.63 and 0.55, respectively. Treatment 1, which involved the use of sodium chloride (not depicted in the graphs), had the highest average dispersed clay with  $77.4 (\pm 3.3)$  mg. The dispersed clay of the treatment that utilized sodium chloride was 5-fold (550%) higher than T0, while it was almost equal (0.36% higher) to T4 which was the second highest treatment with dispersed clay.

Therefore, the higher moisture content observed in the treatments irrigated with higher cation ratio solutions was likely due to clay dispersion. This process can cause a reduction in the number of large pore sizes in the soil and an increase in the number of smaller pores, ultimately leading to less oxygen being available to the plants in the root zone. Therefore, it is important to maintain a proper distribution of large pore sizes in soil to enable adequate water movement, drainage and aeration.

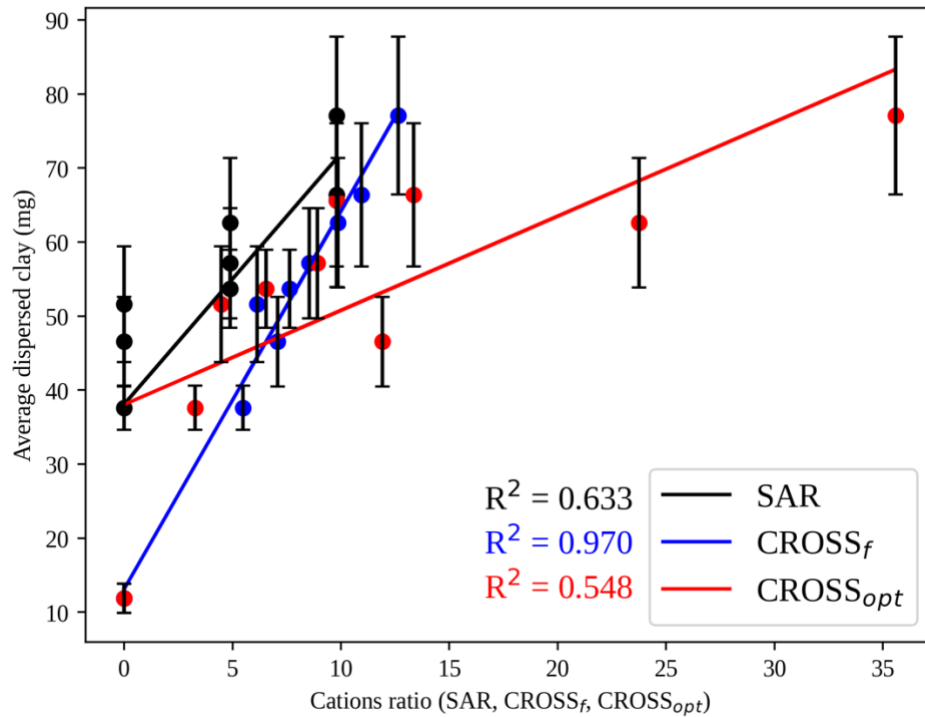


Figure 3.7. Correlation between the average dispersed clay (of the soil samples collected from the pots after terminating the experiment after 40 weeks of irrigation) and cation ratios (SAR, CROSS<sub>f</sub>, CROSS<sub>opt</sub>)

### 3.3.5. Summary of the linear correlation:

Table 3.4 summarizes the linear correlations with and without T0 (gypsum treatment). Based on the summary results, CROSS<sub>f</sub> is a better predictor except for the infiltration correlation, which excludes T0. However, the lack of correlation might be due to the spread of treatments in terms of CROSS<sub>f</sub> values (as shown in Table 3.1). The treatments were intentionally designed to have little spread in terms of CROSS<sub>f</sub> and more spread in terms of CROSS<sub>opt</sub>. Despite the limited spread, moisture content, dispersed clay and permeability were found to be better correlated with CROSS<sub>f</sub>. However, the correlation of CROSS<sub>f</sub> to the infiltration rate is still questionable because infiltration could be impacted by clay dispersion and swelling. Therefore, for low swelling

clayey soils and soils with low clay content,  $CROSS_f$  could be a valid parameter to predict infiltration issues and other related soil physical health indicators.

Table 3.4: Statistical correlations between dispersed clay, moisture content and relative infiltration rate in different recycled water treatments and cation ratios SAR,  $CROSS_f$  and  $CROSS_{opt}$  with and without including treatment that received gypsum (T0).

Indicator	Condition	SAR	$CROSS_f$	$CROSS_d$	$CROSS_{opt}$
Dispersed Clay	R <sup>2</sup> T0 included	0.63	0.97	0.78	0.55
	R <sup>2</sup> T0 excluded	0.8	0.92	0.89	0.59
Moisture Content	R <sup>2</sup> T0 included	0.44	0.63	0.51	0.31
	R <sup>2</sup> T0 excluded	0.36	0.37	0.36	0.2
Infiltration	R <sup>2</sup> T0 included	0.2	0.6	0.4	0.4
	R <sup>2</sup> T0 excluded	0.08	0.14	0.22	0.36

### 3.4. Conclusions:

The common method to assess soil infiltration with respect to the main cations composition in the irrigation water is the sodium adsorption ration (SAR). This relation is valid when the sodium ion is dominant in the water or the soil. However, when potassium exists in the irrigation water with high amount like treated wastewater or in the soil due to fertilizer with high potassium content, SAR usually fails to predict the infiltration issues or other soil physical properties. Two main factors that impacted infiltration is clay dispersion and clay swelling.

The association of sodium cation with clay particles lead to dispersion while potassium lead to both swelling (depending in the clay type) and dispersion. The initial impact of clay dispersion and swelling could appear as good moisture condition for the plants, but the severe reduction in infiltration could happen with long run of the same water quality. Although, both

mechanism occur mostly in the soil surface, the permeability of the water to the deeper layers becomes an issue leading to water logging and hypoxic condition in the rootzone as well as salinity build up in the rootzone due to evaporation and raise up of the groundwater table. Therefore, excess salts in the rootzone will become a challenge to leach away. We found that the proposed new tool which is cation ratio of soil structural stability has better predictability for the infiltration rate, water holding capacity, soil structure and permeability.

## Chapter 4

### Assessing the impact of cation ratios on strawberry growth and development in a greenhouse

#### 4.1. Introduction:

Most plants grow under unsaturated soil conditions. Therefore, available air is as essential as available water. Poor drained soil media usually causes waterlogging. Macropores between aggregates play an important role in improving soil infiltration, aeration and drainage (Scholl et al., 2014). Besides the interaction among cationic composition (Na, K, Ca, Mg) of the applied water, plant roots could improve soil structure by increasing macropores volume. Scholl et al. (2014) studied the hydraulic properties development due to root growth in soil columns. The study revealed a wide range of pore size in the rooted treatment while a narrow range of pore size distribution was observed in the non-rooted columns.

If the soil structure has degraded, the plant growth will be impacted because of waterlogging. The paradox of soil structural degradation on plant growth appears in Farahani et al. (2020) and Chand et al. (2020) studies. Farahani et al. (2020) studied maize growth in pots using field loamy soil. The plants were irrigated by capillary rise with different treatments of Na, K, Ca and Mg solutions (with focus on K:Na ratio) with water EC of 3 and 6 dS/m. The study revealed that micropores, plant available water and plant growth increased with increasing dispersible clay. Chand et al. (2020) investigated the use of recycled water, groundwater and mixed water in tomato grown in a greenhouse experiment using loamy sand soil. The water was applied using drip irrigation. The authors found that tomato yield and growth were higher in the recycled water treatments although it had the highest SAR and CROSS values than the other two

treatments. The highest growth with the recycled water treatment was because the recycled water could contain more nutrients than the other two treatments.

Strawberries are one of the crops most widely irrigated with recycled water in California (PV Water, 2020). Strawberries have high sensitivity toward the salinity of the irrigation water. The maximum salinity level of the soil extract ( $EC_e$ ) should not exceed 4 dS/m (USDA-NRCS, 2013). Depending on the irrigation salinity, a leachate requirement should be applied to avoid salt build-up. On average, strawberry plants require 80 liters/plant/season given that the moisture content is maintained above 50% field capacity (El-Farhan and Pritts, 1997). Therefore, strawberries could have a better response to soil structure alteration than other crops because they require a high amount of water and well-drained soil (Michael Cahn and Belinda Platts, personal communication, 2020). Strawberry growth and development can be evaluated by the start of blooming, earliest fruit harvested, the number of runners, sweetness, fruit size, shoot biomass, branch crown, leaf area and crown injury (Kadir et al., 2006).

The study aimed to assess the response of strawberry growth and development to recycled waters containing different cationic contents of sodium, potassium, calcium and magnesium under a greenhouse environment. The evaluation of strawberry growth and development was based on the yield throughout the growing period, sugar content based on °Brix, plant growth based on plant cover, biomass at the end of the growing period, plant uptake of ions and leachate analysis. In addition, cation ratios were analyzed for correlation with growth, production and biomass.

## 4.2. Methodology:

### 4.2.1. Experimental set up:

Soil was obtained from an agricultural research site located at the University of California Davis, near Davis CA. A soil sample was collected from a depth of 0 to 30 cm, after removing a small layer at the top (5 to 10 cm) that may have had a significant amount of organic matter. The soil had an electrical conductivity ( $EC_e$ ) of 0.95 ( $\pm 0.06$ ) dS/m and a pH of 7.1 ( $\pm 0.53$ ) determined using a saturated paste extract. The soil texture was classified as clay loam, with 35.06% ( $\pm 0.86$ ) sand, 31.56% ( $\pm 1.73$ ) silt and 33.38% ( $\pm 1.25$ ) clay, measured using the hydrometer method. The gravel content was very low, at 0.06% ( $\pm 0.06$ ). The field bulk density was 1.33 ( $\pm 0.09$ ) g/cm<sup>3</sup>, determined by taking undisturbed core samples. The organic carbon content was measured using the loss-on-ignition method and found to be 1.26 ( $\pm 0.08$ ). The exchangeable Na, K, Ca and Mg were determined using inductively coupled plasma atomic emission spectroscopy (ICP-AES), with values of 0.13 ( $\pm 0.01$ ), 0.83 ( $\pm 0.07$ ), 8.27 ( $\pm 0.25$ ) and 11.83 ( $\pm 0.32$ ) meq/100g, respectively. Therefore, the cation exchange capacity (CEC) of the soil was 21.1 ( $\pm 0.53$ ) meq/100g and the exchangeable sodium percentage (ESP) was 0.60% ( $\pm 0.53$ ). The dominant clay mineral in the soil is Montmorillonite (Dasberg and Hopmans, 1992; Lagerwerff and Brower, 1972).

The experiment involved filling pots with soil that had been dried in the air and passed through a 6 mm sieve to achieve a soil structure similar to that of the field. Careful packing of three successive layers was done to achieve an average bulk density of 1.3 g/cm<sup>3</sup>, similar to the field measurement, while minimizing layer-to-layer stratification by shattering the top of each layer. The total water content was determined by measuring the moisture content of the air-dried soil, which was found to be 59.5 mg-water/g-soil ( $\pm 5.0$ , n=15). The study used a total of 176

pots, with four replicates per treatment and four pots per replication. One bare root strawberry (Portola variety) was planted in each pot. Each pot received 45 grams of slow-release fertilizer (15N-9P-12K) required to have optimum non-fertilizer limiting strawberry growth conditions. The fertilizer was mixed at the top with few centimeters of the soil. The lateral and row spacing between the plants was 30 cm. The experiment followed a complete randomized block design, with four blocks and 11 treatments. The experiment was conducted in a greenhouse facility located at University of California, Davis.

#### 4.2.2. Treatment specification:

The treatments used in the study had an electrical conductivity of 1.5 dS/m and were prepared using chloride solutions of sodium, potassium, calcium and/or magnesium, with one exception of a calcium sulfate treatment used to examine the effect of chloride on plants (Table 4.1). The SAR values of the treatments were set at 0, 4.9, 9.8 and infinity (sodium chloride solution). The  $CROSS_f$  and  $CROSS_{opt}$  values of the same treatments ranged from 0 to 12.6 and 0 to 35.6, respectively. The salt content combination in the solutions was designed to ensure treatments with similar SAR values would have varying values of  $CROSS_f$  and  $CROSS_{opt}$ .

In this study, the treatments were administered to the soil in the pots through drip irrigation following two criteria. The first was to maintain a leaching factor of 30%, which ensured that the soil electrical conductivity ( $EC_e$ ) remained below the threshold  $EC_e$  of the strawberry plants which range between range of 1.5-4.0 dS/m (USDA-NRCS, 2013). The second criterion was to keep the tensiometer reading below 10%. MixRite fertilizer injectors were connected with drip line to inject concentrated treatment solutions into the irrigation line resulting in a conductivity of 1.5 dS/m. The soil in the pots was irrigated every day throughout

the 40-week growing period as shown in Figure 4.1. For the first 22 weeks, irrigation was provided in 50 ml pulses every 15 minutes. After this period, the irrigation was increased to 100 ml pulses every 15 minutes. All irrigation was carried out between 11:00 and 13:15 hours.

Table 4.1: Synthetic recycled water chemical composition for various treatments.

Treatments	T0	T1	T2	T3	T4	T5	T6	T7	T8	T9	T10
EC (dS/m)	1.5	1.5	1.5	1.5	1.5	1.5	1.5	1.5	1.5	1.5	1.5
NaCl (mmol/L)	0	15	12	12	12	6	6	6	0	0	0
KCl (mmol/L)	0	0	0	0	0	6	6	6	12	12	12
CaCl <sub>2</sub> (mmol/L)	0	0	1.5	0.75	0	1.5	0.75	0	1.5	0.75	0
MgCl <sub>2</sub> (mmol/L)	0	0	0	0.75	1.5	0	0.75	1.5	0	0.75	1.5
CaSO <sub>4</sub> (mmol/L)	20	0	0	0	0	0	0	0	0	0	0
SAR	0	∞	9.80	9.80	9.80	4.90	4.90	4.90	0	0	0
CROSS <sub>f</sub>	0	∞	9.80	10.95	12.65	7.64	8.54	9.87	5.49	6.13	7.08
CROSS <sub>opt</sub>	0	∞	9.80	13.36	35.59	6.54	8.92	23.75	3.28	4.48	11.92

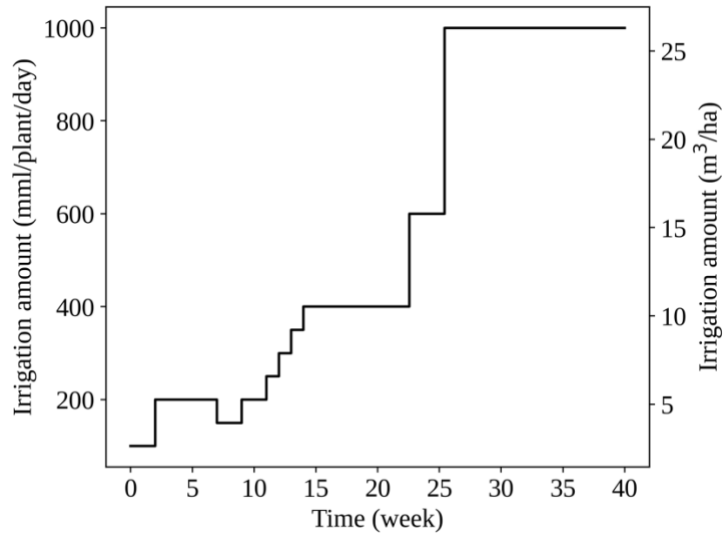


Figure 4.1: Irrigation scheduling based on leaching factor and the tensiometer reading.

#### 4.2.3. Leachate sampling:

A container was positioned under the pots to collect any leachate produced. Leachate was obtained from three pots of each treatment and was subsequently analyzed for EC and pH. Due to cost constraints, only leachate from selected treatments was subjected to chemical analysis for the ions of sodium, potassium, magnesium, calcium and chloride. Treatments 5, 6 and 7 had the highest cationic content and were thus chosen for these analyses. The UC Davis Analytical Laboratory performed the chemical analysis of the leachate using Inductively Coupled Plasma Emission Spectrometry (ICP-AES). The Flow Injection Analyzer Method was employed to analyze the chloride concentration in the leachate.

#### 4.2.4. Quantitative and qualitative analysis of the plant growth and production:

Plant growth and production were analyzed based on plant cover, fruit production and final biomass. To ensure that the mother plant is not affected by the growing runners and weeds, runners were cut and weeds were removed. To measure plant cover, digital images were taken from above the plants every two weeks at approximately the same height to minimize errors in image size relative to the actual plant cover. The Foliage tool (Patrignani, 2020) was then utilized to calculate the relative percentage of green plant cover.

Fruit production was collected and analyzed on a weekly basis. Only fully red fruits were harvested, while any fruits that were not fully red were left to be harvested in the following week. The fruits were classified into two categories: marketable fruits, which weighed more than 10 grams and have no distortion in color or shape and nonmarketable fruits which were less than 10 grams and showed color and/or shape distortion. The fruits were dried in an oven at a

temperature of 60 °C. Both fresh and dry weights of the fruits were recorded as well as the count of each category.

Upon concluding the experiment, the overall plant biomass was assessed. Due to the difficulty in separating roots from the soil, they were not included in the total biomass evaluation. The biomass weight was recorded both fresh and dry. The plants were dried in an oven at a temperature of 60 °C.

#### 4.2.5. Plant and fruit content analysis:

Plants and fruits were evaluated for their content. Fruits were evaluated for their sugar content using Portable Optical Refractometer and expressed as °Brix. This evaluation was conducted at various time points throughout the growing period. Marketable fruits were selected to obtain a representative sugar content.

At the end of the experiment, in week 41, the entire plants of each treatment in each block (including the crown, leaves, flowers and fruits) were dried and grounded to measure their ions content uptake. The specific ions analyzed were sodium, potassium, calcium, magnesium and chloride. This measurement was used to understand the relative uptake from the solution as well as the slow-release fertilizer. The sodium, potassium, calcium and magnesium were quantitatively estimated using a nitric acid/hydrogen peroxide microwave digestion and then measured using ICP-AES. For chloride analysis, a water extraction technique was used and the analysis was performed by ion chromatography (IC) with conductivity detection.

#### 4.2.6. Statistical analysis:

A one-way Analysis of the variance (ANOVA) was conducted to determine statistical significance. ANOVA is appropriate when the data satisfy the assumptions of linearity, uniformly distribution and homogeneity. In case where some observations do not meet these assumptions, a transformation was applied to the data to address the issue.

Statistical significance was considered achieved when the p-value was less than 0.05 or when the confidence interval is 95%. To further analyze and compare treatments Tukey HSD (Honestly Significant Difference) test was performed, evaluating the treatments in pairs. This test helps identify which treatment groups differ significantly from one another.

To evaluate the cation ratios equations (Equation 1, 2 and 3) on plant growth and production, a linear regression analysis was conducted to calculate the coefficient of determination ( $R^2$ ). Sodium adsorption ratio (SAR) and cation ratio of soil structural stability ( $CROSS_f$  and  $CROSS_{opt}$ ) were chosen for this evaluation. SAR (Equation 1) is a commonly used parameter to assess the physical health of soil particularly for predicting changes in infiltration rate (Richards, 1954).  $CROSS_f$  (Equation 2) was found to be a better predictor than SAR for soil structure changes measured as spontaneous dispersible clay with an  $R^2$  value of 0.95 (Rengasamy and Marchuk, 2011). While  $CROSS_{opt}$  (Equation 3) demonstrated a high level of prediction accuracy for the threshold electrolyte concentration with an  $R^2$  value of 0.95 (Smith et al., 2015).

$$SAR = \frac{Na^+}{\sqrt{Ca^{2+} + Mg^{2+}}} \quad 4.1$$

$$CROSS_f = \frac{Na^+ + 0.56 * K^+}{\sqrt{Ca^{2+} + 0.60 * Mg^{2+}}} \quad 4.2$$

$$CROSS_{opt} = \frac{Na^+ + 0.335 * K^+}{\sqrt{Ca^{2+} + 0.0758 * Mg^{2+}}} \quad 4.3$$

where  $\text{Na}^+$ ,  $\text{K}^+$ ,  $\text{Ca}^{2+}$  and  $\text{Mg}^{2+}$  are the concentrations of the ions in mmol/L.

### 4.3. Results and Discussion:

#### 4.3.1. Leachate analyses:

Cation concentration (Na, K, Ca, Mg and Cl) in the leachate is shown in Figure 4.2. Each data point (in Figures 4.2b to 4.2f) represents the concentration of three mixed solution samples from different pots and replications of the same treatment. Not all treatments were analyzed due to the high cost of the analyses. Treatments 5, 6 and 7 which had the most cations in their solutions were selected for the leachate analyses. From week 9 to week 15, the volume of the leachate solution was not sufficient for laboratory analysis. In week 15, the solution was very little and it was concentrated.

Figure 4.2a illustrates the average of the ion concentrations in the leachate for treatments T5, T6 and T7. The shaded area represents the standard error around the mean. Among the ions measured, the highest concentration in the leachate was observed in week 15 for the chloride with average 148 mmol/L. The higher concentration can be attributed to the use of chloride salts in preparing the treatment solutions. The significant amount of chloride leaching from the soil indicates that chloride is easily mobilized and washed away through the leaching process. Sodium and calcium displayed similar concentration in the leachate, around 25 mmol/L, while magnesium was 58 mmol/L.

The gradual increase of the irrigation amount (Figure 4.1) was effective in reducing the ion concentrations in the leachate over time. However, the leaching rate for sodium between week 15 and week 25 was relatively slower compared to calcium, magnesium and chloride

indicating that sodium was not easily leached from the soil (Figure 4.2). The rate of leaching the ions between the weeks 15 to 25 are in the order of  $Cl > Mg > Ca > Na$ .

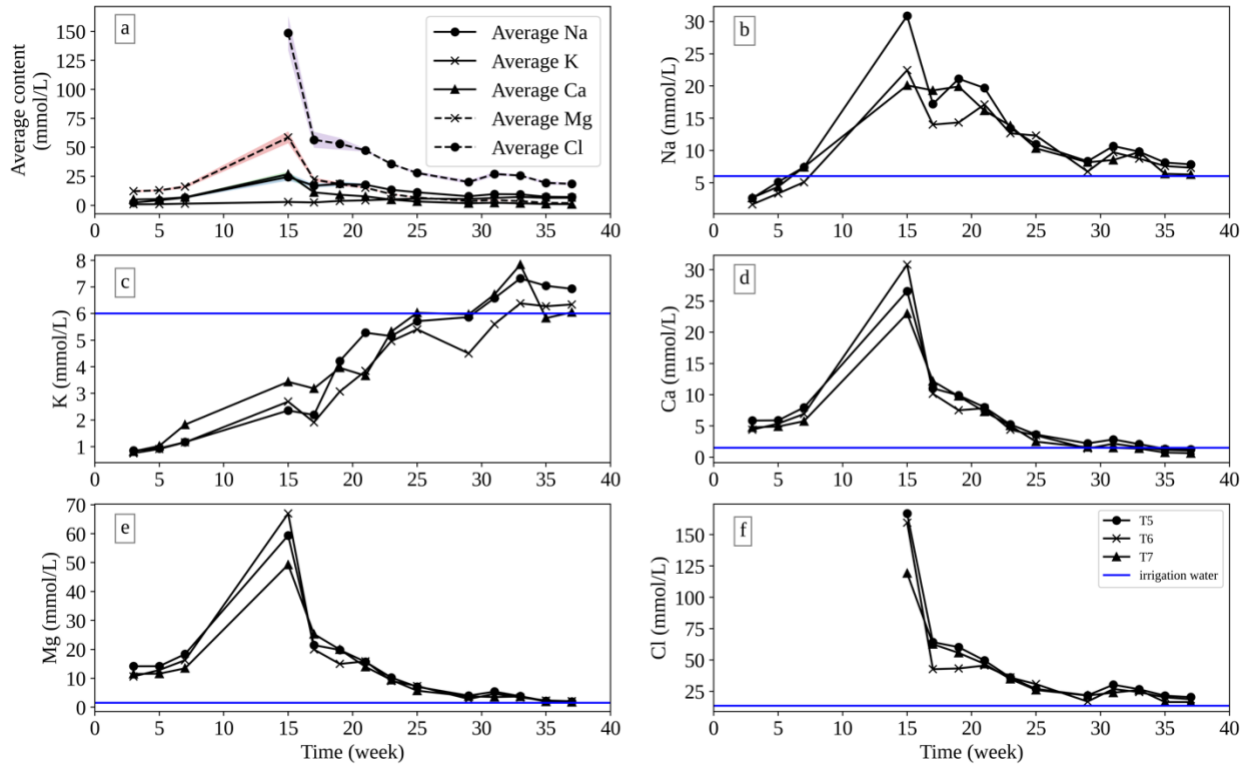


Figure 4.2: Leachate ion concentrations in synthetic recycled water for treatments T5, T6 and T7 in a greenhouse strawberry experiment: a) average concentration combining T5, T6 and T7, and the shaded area represents the standard error; b) sodium concentration; c) potassium concentration; d) calcium concentration; e) magnesium concentration; f) chloride concentration. The blue line in each graph indicates the concentration of the ion in the treatment solutions. Each dot in graphs b-f represents three mixed leachate samples collected from different blocks for the same treatment.

The potassium dynamic exhibited, however, a distinct trend compared to the other ions. Most likely, potassium was trapped within the clay particles. After increasing the irrigation amount, potassium concentration gradually increased until it reached the level present in the irrigation solution. These findings provide insights into the leaching behavior of different ions in the soil under the specific experimental conditions. Understanding these processes can be beneficial for optimizing irrigation practices and nutrient management to support healthy plant growth and sustainable agricultural practices when using water of marginal quality.

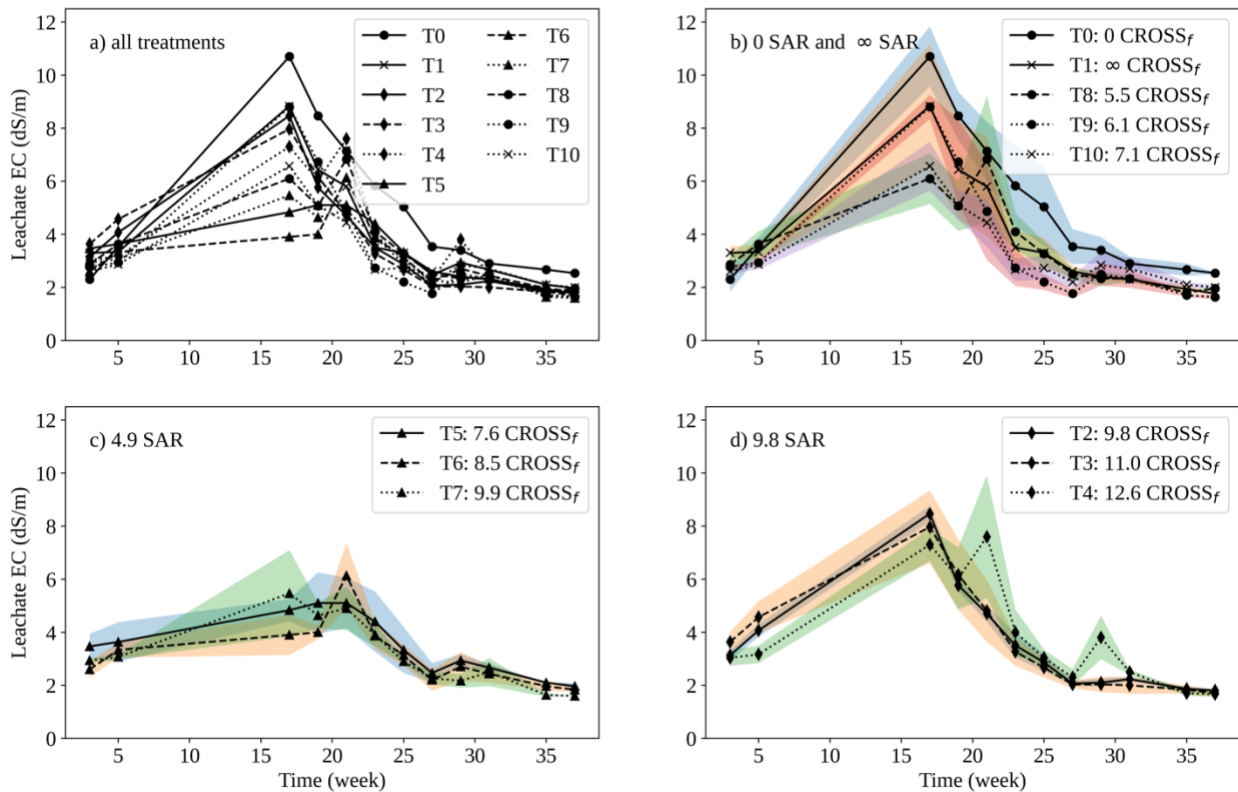


Figure 4.3: Average electrical conductivity (dS/m) of the leachate over the growing period where: a) all treatments; b) 0-SAR and infinity SAR treatments; c) 4.9-SAR treatments; d) 9.8-SAR treatments. The shaded area represents the standard error.

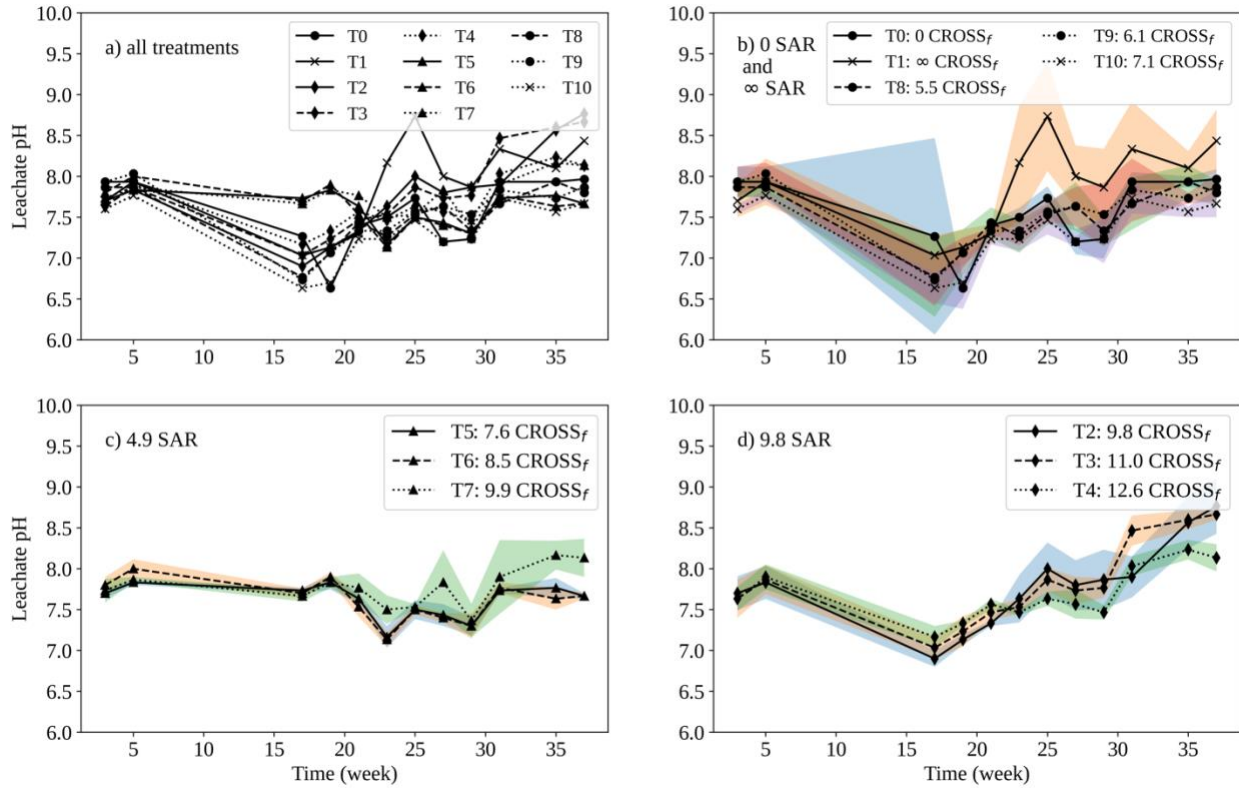


Figure 4.4: Average pH of the leachate over the growing period where: a) all treatments; b) 0-SAR and infinity SAR treatments; c) 4.9-SAR treatments; d) 9.8-SAR treatments. The shaded area represents the standard error.

Figure 4.3 and Figure 4.4 depict the average electrical conductivity (EC) and pH values of the collected leachate throughout the growing period. The shaded area in the figures represents the standard error. There were insufficient solutions between the week 9 to 15 to accurately represent the EC and pH. After this gap, the solution became more concentrated, leading to higher EC values in the leachate. Following the increase in irrigation amount after week 15, the leachate volume increased, consequently, the EC of the leachate gradually decreased to approximately 2 dS/m for all treatments. The pH slightly dropped from pH 8 for the treatments with zero and 9.8 SAR to around pH 7. Subsequently, it started to raise gradually,

reaching approximately pH 8. While for the 4.9 SAR treatments group, pH remained relatively stable, ranging between pH 7.5 and pH 8.

#### 4.3.2. Plant growth based on plant cover:

Figure 4.5 illustrates plant growth based on plant cover. It is evident that plants reach their maximum size or density during the initial ten weeks of the growing period. From week 10 to week 30, the impact of the treatments on plant growth appears to diminish and there was no observed statistical difference within most of the treatments to make a confident decision. This might be attributed to the accumulation of salts (Figure 4.2 and 4.3) in the soil which enhances the infiltration rate due to the salinity's influence on soil physical properties. However, after increasing the irrigation water to the maximum irrigation dose (Figure 4.1) after week 25, the effect of the treatments become more apparent.

Table 4.2 presents the results of the statistical analysis using the Tukey HSD test with a significance level of 0.05 from the period of week 30 to week 40. Treatments with similar letters indicate no statistically significant difference, whereas treatments with different letters are statistically significant from each other. Treatments T0 and T1 represented the two extreme conditions with T0 involving a gypsum solution and T1 utilizing sodium solutions. Both treatments showed statistical significance and were significantly different from all other treatments. T0 exhibited the highest least square mean while T1 had the lowest and the remaining treatments fell in between. Although treatments T0, T8, T9 and T10 all had a SAR of 0 (Figure 4.5b), T0 was statistically different from T8, T9 and T10. This implies that the effect of potassium on infiltration rate should be considered, as T0 displayed improved growth compared to the other treatments with 0 SAR (T8, T9 and T10). However, no statistical significance was

observed among treatments T8, T9 and T10. A Similar observation can be made for the 4.9 SAR group (Figure 4.5c) which includes treatments T5, T6 and T7. Although all these treatments had a SAR value of 4.9, they were still statistically significant from each other. Moving on to the 9.8 SAR group (Figure 4.5d), treatments T2 and T4 were not statistically different from each other but they were significantly different from T3.

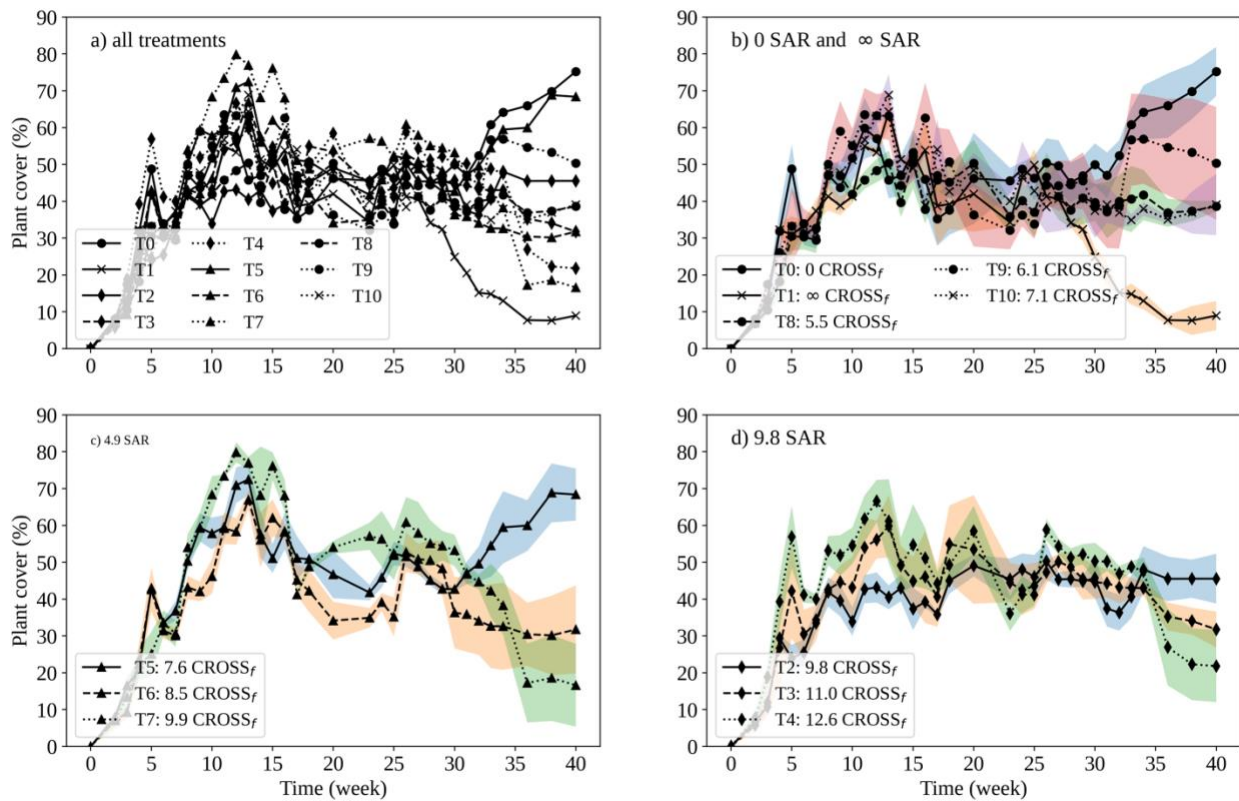


Figure 4.5: Plant weekly growth based on average plant cover using Foliage tool where: a) all treatments; b) 0-SAR and infinity SAR treatments; c) 4.9-SAR treatments; d) 9.8-SAR treatments. The shaded area represents the standard error.

Table 4.2: Tukey HSD test for the plant cover from week 30 to week 40. Similar letters indicate no statistical difference. The treatments are arranged in descending order of the average plant cover at  $P < 0.05$ .

Treatment		Least Sq Mean
T0	A	57.6
T5	B	49.8
T10	B C	46.3
T9	B C	45.2
T8	B C D	44.4
T2	C D	42.4
T6	C D	41.8
T4	D	38.8
T7	E	31.3
T3	E	30.0
T1	F	16.8

#### 4.3.3. Yield analysis:

Some plants started to bloom in week 2. The first harvest began in week 6. By week 13, all treatments were producing fruits and continued to do so until the end of the experiment. Table 4.3 presents the summary of the yield production for the entire experiment. The total dry matter of the strawberries was around 8% of the total fresh weight, indicating that 92% of their composition was water. Around 23% of the total production was marketable fruits. Figure 4.6 illustrates the relationship between fresh and dry weight along with the corresponding equation that could help in estimating the dry weight of the fruits from their fresh weight considering that the fruits were dried at 60 °C.

Table 4.3: Summary of harvested fruits from strawberry plants in the greenhouse experiment.

Parameter	Value ( $\pm$ standard error)
Total fresh (kg)	143.81
Total dry (kg)	11.58
Average fresh (kg) n=4	35.95 ( $\pm$ 3.10)
Average dry (kg) n=4	2.90 ( $\pm$ 0.27)
Total marketable fresh (kg)	33.01
Total marketable dry (kg)	2.66
Average marketable fresh (kg) n=4	8.25 ( $\pm$ 1.23)
Average marketable dry (kg) n=4	0.67 ( $\pm$ 0.11)
Total count	20967
Total marketable count	2556

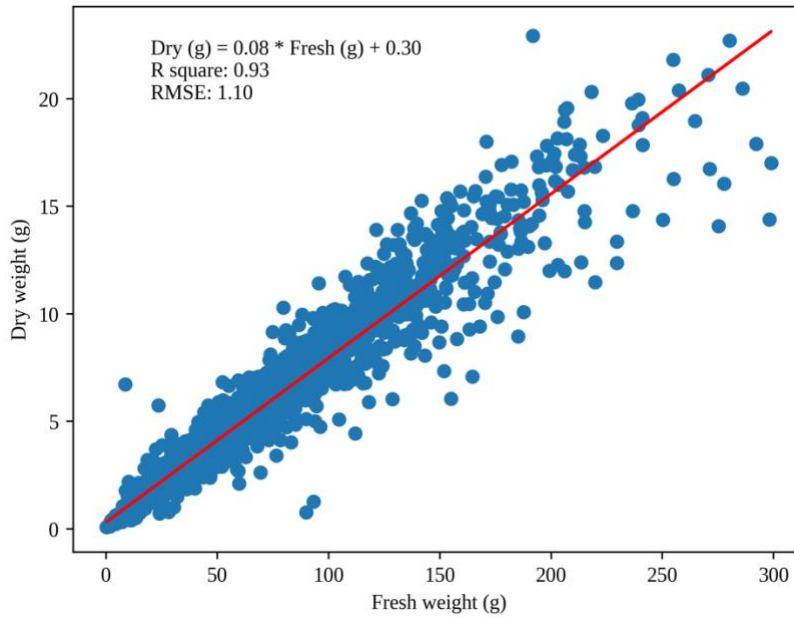


Figure 4.6: empirical model of fresh-dry fruit weight for the entire experiment.

The weekly fruit production is shown in Figure 4.7. Overall, the maximum production occurred in week 17 with an average of 225 g per treatment. However, it subsequently decreased to an average of around 75 g per treatment in week 22. When considering the entire yield of the experiment, no statistically significant differences were observed among most of the treatments,

making it difficult to confidently determine the yield variations. Therefore, to further analyze the yield in relation to the treatments, the statistical analysis of the plant cover was used to analyze the yield with respect to the treatments for the period from week 30 to week 40.

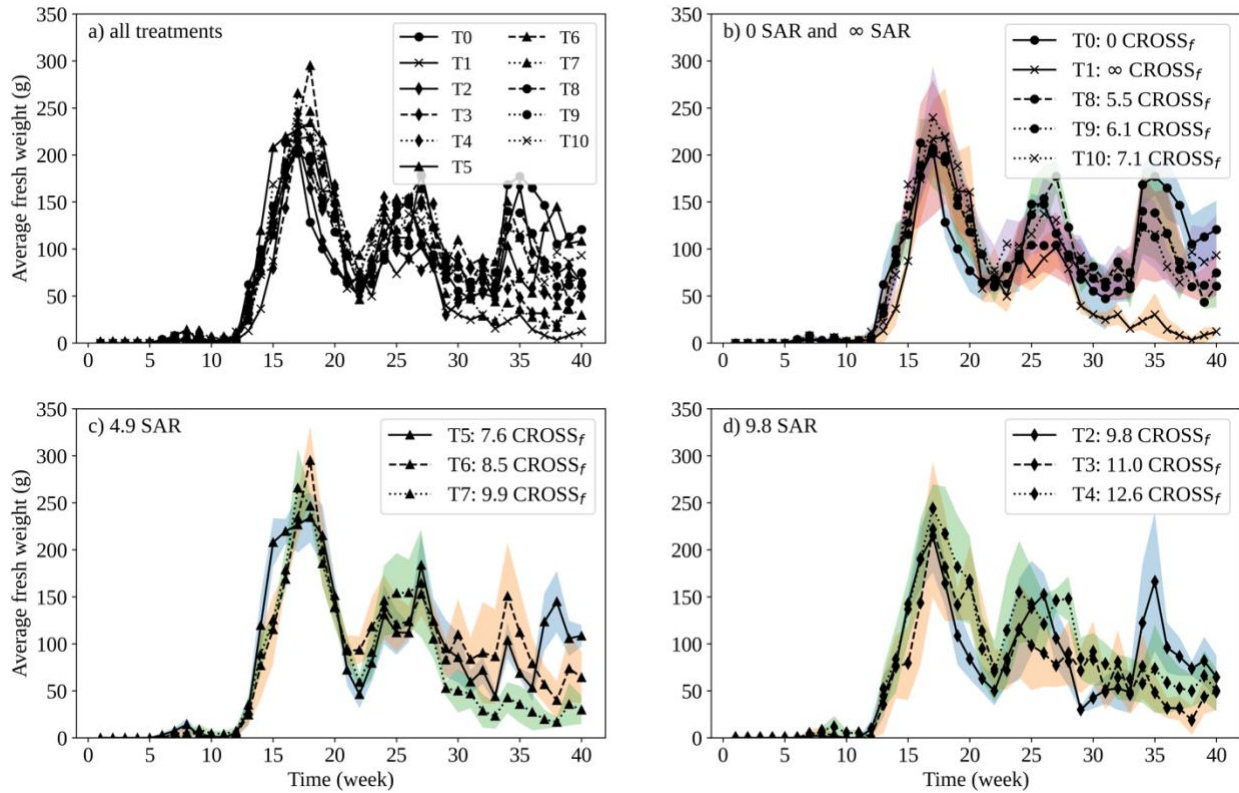


Figure 4.7: Average weekly fruit production where: a) all treatments; b) 0-SAR and infinity SAR treatments; c) 4.9-SAR treatments; d) 9.8-SAR treatments. The shaded area represents the standard error.

Figure 4.8a displays the average fresh production from week 30 to 40, while Figure 4.8b exhibits the average marketable fresh production during the same period. The correlation analysis of the average fruit production (Figure 4.8c) and the average marketable fresh production (Figure 4.8d) from week 30 to week 40 indicated that the production showed stronger correlation with CROSS<sub>f</sub> than SAR and CROSS<sub>opt</sub>. The R<sup>2</sup> of 0.56 for the average fruit

production and 0.58 for the marketable fruit fresh production. This result suggests that the changes in soil physical properties have an impact on both plant growth and yield production.

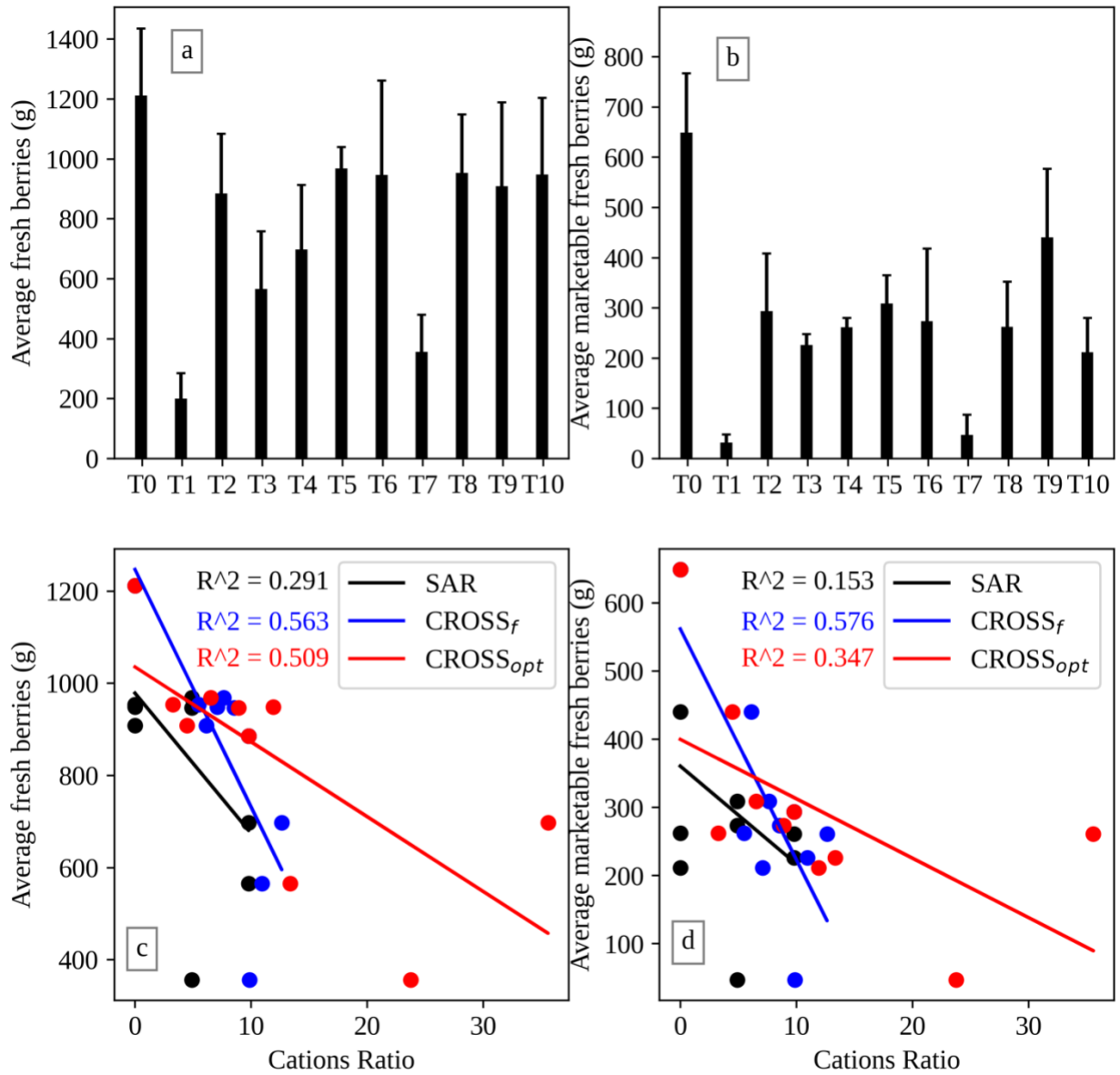


Figure 4.8: Average total harvested fruits between weeks 30 to 40 and corresponding correlations with the cation ratios: a) Average fresh weight of the harvested fruits; b) Average fresh weight of the harvested marketable fruits; c) correlations of SAR,  $CROSS_f$  and  $CROSS_{opt}$  with the average fresh weight of the harvested fruits; d) correlations of SAR,  $CROSS_f$  and  $CROSS_{opt}$  with the average fresh weight of the harvested marketable fruits.

#### 4.3.4. Sugar content based on °Brix:

The sugar content of the harvested fruits is presented in a box plot graph in Figure 4.9. On average, the sugar content was 8.0 ( $\pm 0.2$ ) °Brix. Although no specific trend was observed concerning the cation ratios, the ANOVA demonstrated statistical significance with a  $p$ -value  $< 0.05$ . Specifically, T1 exhibited a higher observed sugar content than all other treatments. The Tukey HSD analysis indicated that T1 (9.6 °Brix) was statistically significant when compared to T0 (7.1 °Brix) and T10 (7.0 °Brix). However, it did not show statistical significance when compared to the rest of the treatments (8.0 °Brix). Therefore, the 22% increase in °Brix as compared to the overall average (7.8 °Brix, excluding T1) suggests that sodium enhances the sweetness of the strawberry fruits.

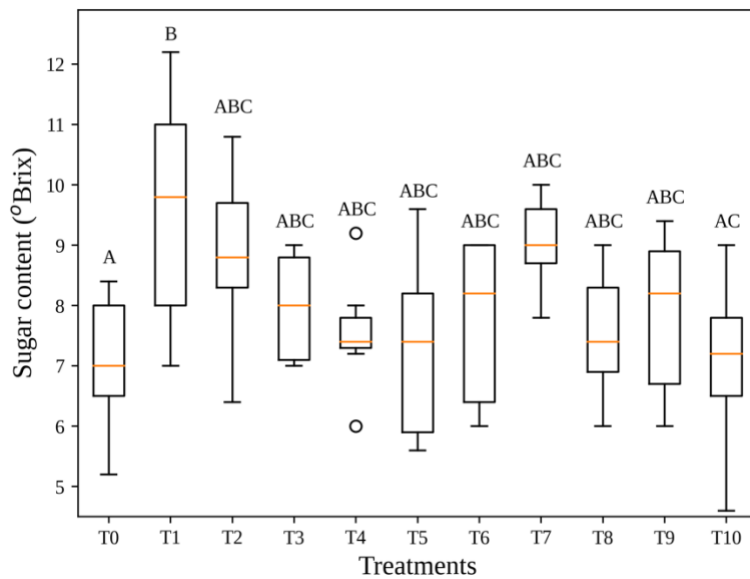


Figure 4.9: Box plot of the sugar content of the fruits measured as °Brix at different weeks.

Letters indicate the statistical significance where similar letters are not statistically significant while different letters are statistically significant at  $P < 0.05$ .

#### 4.3.5. Biomass and plant cover at the end of the experiment:

Figure 4.10 shows results of the average strawberry fresh and dry biomass collected at the end of the greenhouse experiment as well as the final plant cover. The error bars represent the standard error of the mean. The subsequent correlation between the average fresh biomass and dry biomass with plant cover was 0.94 and 0.81, respectively. The correlation between the average plant biomass and the plant cover with the cation ratios (SAR,  $CROSS_f$ ,  $CROSS_{opt}$ ) for the different recycled water qualities showed the highest correlation with  $CROSS_f$  followed by SAR and the least correlation with  $CROSS_{opt}$  (Table 4.4). It is worth noting that Treatment 1 had the lowest average biomass probably due to reduced drainage within the pots affecting oxygen levels. Overall, the results indicate that increasing sodicity resulted in reduced strawberry productivity.

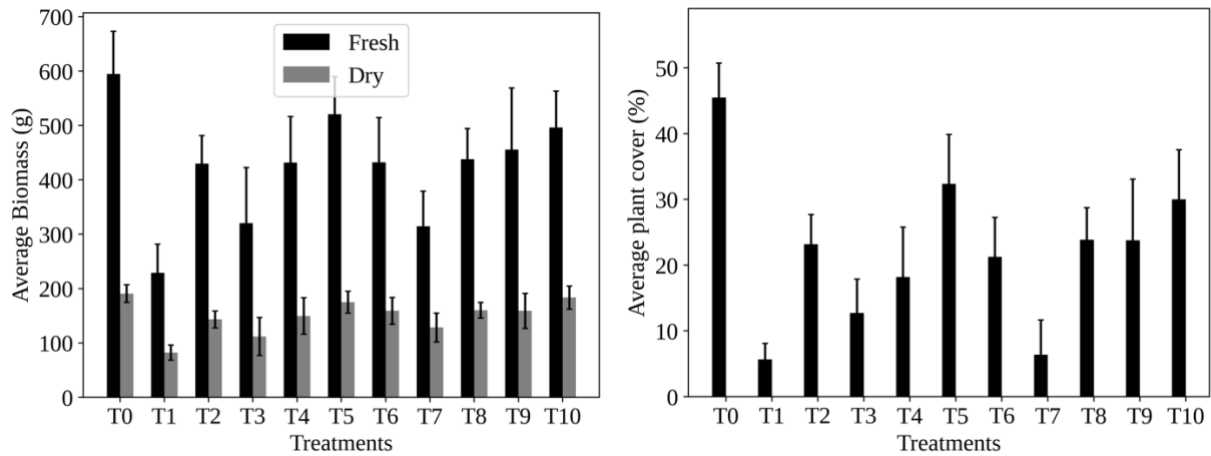


Figure 4.10: a) Average fresh and dry biomass of the whole plants and b) average plant cover at the end of the experiment.

Table 4.4: Coefficient of determinations ( $R^2$ ) of the Correlation between the average biomass and plant cover at the end of the experiment with SAR,  $CROSS_f$  and  $CROSS_{opt}$

Parameter	SAR	$CROSS_f$	$CROSS_{opt}$
Average fresh biomass (g)	0.29	0.55	0.27
Average dry biomass (g)	0.48	0.53	0.23
Average plant cover (%)	0.30	0.67	0.47

#### 4.3.6. Analysis of the plant content:

Strawberry salt uptake in the form of total sodium, potassium, calcium, magnesium and chloride is shown in Figure 4.11. All treatments demonstrated consistency with the cation composition of the applied recycled water. Tukey HSD statistical test was conducted on the data by grouping the treatments based on their similar cationic content. For instance, treatments T2, T5 and T8, which had 0-magnesium in their solution, were compared with treatments T3, T6 and T9 (0.75-magnesium) as well as treatments T4, T7 and T10 (1.5-magnesium), in terms of magnesium content in the plant tissue. Similar analyses were performed for the sodium, potassium and calcium content. The results revealed statistically significant differences among all the groups with p-values less than 0.05.

For sodium, we observed that plants irrigated without sodium solutions (T0, T8, T9, T10) had no sodium in their plant tissue. The sodium content in the plant tissues increased with increasing sodium in the recycled water solution until the maximum with the treatment 1 (sodium solution). The result of the sodium uptake by the plants irrigated with sodium solution only (T1) probably indicates the maximum sodium that strawberry plants can uptake (Figure 4.11b).

For potassium (Figure 4.11c), plants that were irrigated with zero potassium in solution (T0-T4) had the lowest potassium content in plant tissues with 1.38 ( $\pm 0.09$ )%. Therefore, the

amount of potassium in the plant tissues must have come from the slow-release fertilizer or residual potassium in the soil. The rest of the plants had higher potassium concentrations in their plant tissues and that extra accumulation must have come from the potassium in the synthetic recycled water solutions. Treatments T5, T6 and T7 had potassium of 6 mmol/L in their irrigation solution resulting in an observed potassium content of 2.83 ( $\pm 0.06$ )% which was double that of the zero-potassium solutions. Therefore, irrigating with potassium-rich water allows for the use of a non-potassium fertilizer while still achieving similar effects to those observed with potassium-containing fertilizer. On the other hand, treatments T8, T9 and T10 were subjected to a potassium concentration of 12 mmol/L in their solution, twice the amount used in treatments T5, T6 and T7. Despite this doubling of potassium concentration, the increase in potassium content in the plant tissue was only 42% compared to T5, T6 and T7. Additionally, it was approximately 200% higher than the treatments that lacked potassium in their solution.

The maximum observed calcium content in the plant tissue was found in T0 (the gypsum solution treatment) with 2.4 ( $\pm 0.2$ )% (Figure 4.11d). Conversely, treatments T1, T4, T7 and T10 had the minimum observed calcium due to the use of a non-calcium solution. As a result, the observed calcium content in the plant tissue was from the slow-release fertilizer and amounted to 0.91 ( $\pm 0.05$ )%. A similar trend was observed for the magnesium with minimum observed magnesium found in T0, T1, T2, T5 and T8 averaging at 0.53 ( $\pm 0.01$ )% which is likely attributed to the slow-release fertilizer (Figure 4.11e). As the calcium and magnesium content in the solution increased, the calcium and magnesium content in the plant tissue also increased.

It should be noted that the uptake of magnesium and calcium slightly decreased as the potassium in the irrigation water increased. For instance, treatments T2, T5 and T8 received similar calcium content in their solution, however, the calcium content in the plant tissue

followed the order  $T2 > T5 > T8$  which is opposite to the order of potassium content  $T2 < T5 < T8$ . To compare the treatments with 0-potassium, 6-potassium and 12-potassium, a Tukey HSD test was conducted. Since the calcium content differed between the treatments with similar potassium content, the calcium content was normalized for the Tukey HSD test. The normalized calcium content in the 0-potassium treatments (T2, T3 and T4) was statistically significant compared to the 6-potassium treatments and it was also statistically significant compared to the 12-potassium treatments. However, the 6-potassium treatments did not show statistically significant differences compared to the 12-potassium treatments. In the case of magnesium, treatments T4, T7 and T10 received similar magnesium content in their solution, however, the magnesium content in the plant tissue followed the order  $T4 > T7 > T10$  which was opposite to the order of potassium content. After normalizing the magnesium content in the plant tissue with respect to the potassium dose in the solution, the Tukey HSD analysis showed statistical significance between the 0-potassium treatments and the 12-potassium treatments as well as between the 6-potassium treatments and the 12-potassium treatments. However, there was no statistical significance between the 0-potassium treatments group and the 6-potassium treatments group in terms of their magnesium content in the plant tissue.

The gypsum treatment (T0) resulted in plants with a minimal chloride content in the biomass, about  $0.18 (\pm 0.02)\%$ . This amount could be attributed to the residual chlorine present in the water used to prepare the solutions. However, the remaining treatments exhibited a significantly substantial chloride content in the plant tissue, approximately  $2.93 (\pm 0.06)\%$  due to chloride-based salts used to create the various treatments of synthetic recycled water. It is important to note that elevated levels of chloride in strawberries can lead to chloride toxicity.

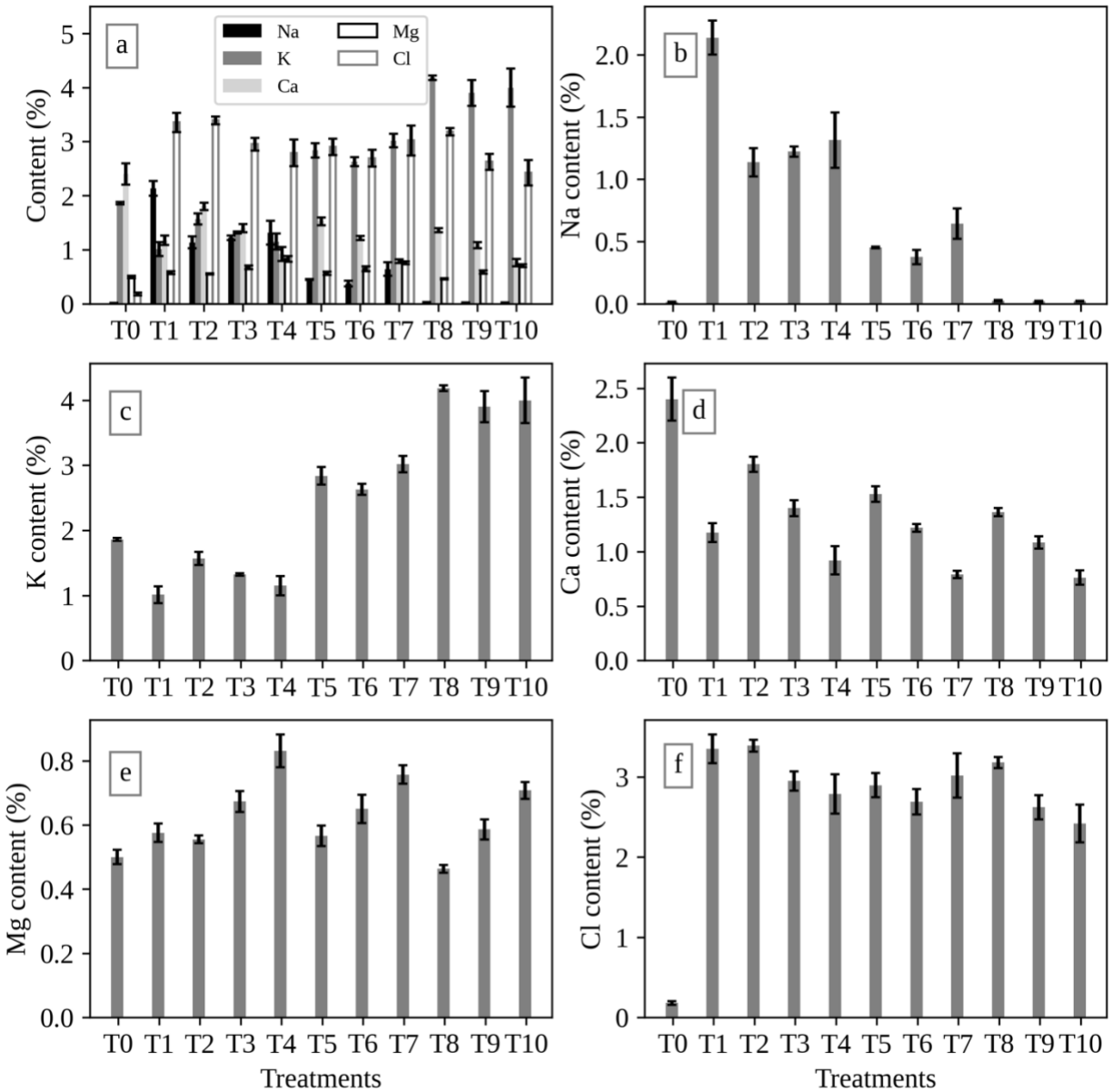


Figure 4.11. Average cation content in the plant tissues of various synthetic recycled water irrigation treatments (T0 to T10 defined in Table 4.1) measured at the end of the experiment after drying and grinding the plants: a) relative ions content; b) sodium content; c) potassium content; d) calcium content; e) magnesium content; f) chloride content.

#### 4.4. Conclusions:

Most plants grow in unsaturated soil condition. Soil structure degradation due to high monovalent cations to divalent cations ratio could lead to pore clogging by clay dispersion. Generally, natural water does not cause this issue. However, low-quality waters like treated wastewater may contain varying concentrations of cations. The common standard used to evaluate the sodicity effect is the sodium adsorption ratio (SAR). Nevertheless, the newly proposed standard, the cation ratio of soil structure stability (CROSS), could be a better predictor of sodicity impact.  $CROSS_f$  was found to be a better predictor for soil structure (measured as spontaneous dispersible clay) and  $CROSS_{opt}$  was found to be a better predictor for the threshold electrolyte concentration.

The paper presents the growth and production of strawberry plants in greenhouse condition. The plants were irrigated with 11 synthetic recycled water treatments. Four of the treatments had zero SAR value, three had 4.9 SAR, three had 9.8 SAR and one treatment had sodium solution. By varying the sodium, potassium, calcium and magnesium content in the treatments' solution, the same treatments had  $CROSS_f$  ranging between 0 and 12.6 and  $CROSS_{opt}$  ranging between 0 and 35.6.

The statistical analysis of the plant growth showed statistically significant differences between treatments of similar SAR values. Subsequent analysis of the fruit production revealed that fruit production decreased with increasing cation ratios (SAR,  $CROSS_f$  and  $CROSS_{opt}$ ).  $CROSS_f$  showed a stronger correlation with fruit production compared to SAR and  $CROSS_{opt}$ . Similarly, the analysis of plant biomass and plant cover at the end of the experiment demonstrated reduced plant growth with increasing cation ratios, with better correlation with respect to  $CROSS_f$ .

The plants were analyzed for their content in terms of sodium, potassium, calcium, magnesium and chloride. The results were statistically significant and consistent with the ion content in the solution treatments. It was concluded that salts added to the solution were observed in the plant tissue, which could raise implication for human health when consuming such product. The plant content analysis showed that the uptake of calcium and magnesium by the plant could be reduced as the potassium content in the solution increased.

## Chapter 5

### Conclusions and Recommendation

In this study, two main experiments were conducted: the soil column experiment and the greenhouse experiment. The purpose of the study was to assess the established models used to evaluate water quality in relation to soil physical properties specifically the sodium adsorption ratio (SAR) and the cation ratio of structural stability (CROSS). The two primary properties under examination were the infiltration rate and soil aggregate stability. The conclusion drawn from both experiments is that CROSS<sub>f</sub> could potentially offer enhanced accuracy and understanding of soil infiltration rate and soil aggregate stability. Consequently, it may serve as a more effective benchmark for predicting the impact of sodicity compared to SAR.

In the soil column experiment, a set of thirty columns were conducted using field soil that was characterized by a clay loam texture. A comprehensive evaluation was conducted on these columns to examine their soil structure and saturated hydraulic conductivity. The irrigation process involved the regular application of water to the soil columns, maintaining a constant water head of 1 cm after pre-saturation. The salinity of the used solution remained constant at 1.5 dS/m. In contrast to SAR, the results revealed a strong association between CROSS and both saturated hydraulic conductivity and soil aggregate stability. The coefficients of determination for hydraulic conductivity and soil structure were 0.90 and 0.94 for CROSS, respectively, and 0.75 and 0.78 for SAR. Furthermore, clay dispersion was investigated at various depths. Notably, treatments with 0-SAR values but potassium in their solutions had significantly more dispersible clay than the calcium chloride treatment, across the entire soil column which was 53 cm.

For the greenhouse experiment, eleven treatments were prepared with an electrical conductivity (EC) of 1.5 dS/m and varying values in terms of cation ratio models. The analysis of soil properties included a permeability test, an infiltration test using the Wooding Infiltrometer, soil moisture content measured by a TDR sensor and clay dispersion evaluated using the spontaneous dispersible clay method. The treatment that utilized sodium chloride exhibited the lowest average infiltration rate. The infiltration rate decreased with increasing SAR and  $CROSS_f$ , however,  $CROSS_f$  better predicted the reduction in infiltration compared to SAR. The results demonstrated a stronger correlation with  $CROSS_f$  yielding an  $R^2$  value of 0.6, in contrast to SAR with an  $R^2$  value of 0.2 as observed through correlation with the average relative infiltration rate. Moisture content analysis indicated that degraded soil retained water for longer periods than aggregated soils. Among the treatments, the sodium chloride treatment exhibited the highest measured moisture content after 7 days since irrigation was terminated. The correlation of the measured moisture content showed a stronger association with  $CROSS_f$  achieving an  $R^2$  value of 0.63 as opposed to SAR with an  $R^2$  value of 0.44.

For the analysis of plant growth and development in the greenhouse experiment, various parameters were examined. These included growth based on plant cover, fruit production, biomass at the experiment's conclusion, fruit sugar content measured as °Brix and plant tissue content. The analysis revealed that plant biomass and plant cover at the end of the experiment demonstrated reduced growth with increasing cation ratios. Better correlations were observed with  $CROSS_f$ , yielding  $R^2$  values of 0.55 for biomass and 0.67 for plant cover, along with SAR correlations of  $R^2$  0.29 and  $R^2$  0.30, respectively. Similarly,  $CROSS_f$  exhibited a stronger correlation with fruit production ( $R^2$  0.56) compared to SAR ( $R^2$  0.29). No specific trend was observed for °Brix and the average across all treatments was 0.8 ( $\pm 0.2$ ). Plant content

consistently aligned with the applied treatments. The maximum observed levels of Na, K, Mg, Ca and Cl in the strawberry plant tissue were 21, 40, 7.7, 24 and 29 parts per thousand, respectively. In contrast, the maximum observed content attributed to the slow-release fertilizer was 0 (due to the absence of sodium), 14, 5.3, 9.1 and 0 parts per thousand for Na, K, Mg, Ca and Cl, respectively. Plant content analysis indicated that the uptake of calcium and magnesium by the plant could be reduced as the potassium content in the solution increased.

The cation ratio models were compared under two different experimental conditions. The soil column was only run under bare soil conditions and with a continuous supply of irrigation. The greenhouse experiment was conducted using drip irrigation and strawberry plants were planted introducing the effect of roots on the soil. Additionally, fertilizer was added to the soil to promote plant growth. In both experiments, the infiltration rate and soil structure were evaluated. Plant growth and production were further analyzed in the greenhouse experiment. Both experiments concluded with a consistent finding that  $CROSS_f$  could be a better replacement than SAR. It was recommended that treatments be designed such that the values of  $CROSS_f$  have more spread at a given SAR. This could improve the statistical analysis output. Additionally, it is worth comparing the two models with soil that has different than montmorillonite clay mineralogy which was the condition of the soil used in this study.

## References

- Ahmed, S., Swindale, L.D., El-Swaify, S.A., 1969. Effects of Adsorbed Cations on Physical Properties of Tropical Red Earths and Tropical Black Earths. *J. Soil Sci.* 20, 255–268. <https://doi.org/10.1111/j.1365-2389.1969.tb01572.x>
- Aldughaisi, U., Grattan, S., Kisekka, I., 2024. Assessing the impact of cation ratios on strawberry growth and development in a greenhouse. Under preparation.
- Amezketta, E., Aragües, R., Gazol, R., 2004. Infiltration of water in disturbed soil columns as affected by clay dispersion and aggregate slaking. *Spanish J. Agric. Res.* 2, 459. <https://doi.org/10.5424/sjar/2004023-100>
- Arienzo, M., Christen, E.W., Jayawardane, N.S., Quayle, W.C., 2012. The relative effects of sodium and potassium on soil hydraulic conductivity and implications for winery wastewater management. *Geoderma* 173–174, 303–310. <https://doi.org/10.1016/j.geoderma.2011.12.012>
- Arienzo, M., Christen, E.W., Quayle, W., Kumar, A., 2009. A review of the fate of potassium in the soil-plant system after land application of wastewaters. *J. Hazard. Mater.* 164, 415–422. <https://doi.org/10.1016/j.jhazmat.2008.08.095>
- Ayers, R.S., Westcot, D.W., 1985. Water quality for agriculture. Food and Agriculture Organization of the United Nations Rome.
- Buelow, M.C., Steenwerth, K., Parikh, S.J., 2015. The effect of mineral-ion interactions on soil hydraulic conductivity. *Agric. Water Manag.* 152, 277–285.
- Cecconi, S., Salazarand, A., Martelli, M., 1963. The effect of different cations on the structural stability of some soils. *Agrochimica* 7, 185–204.
- Chand, J., Hewa, G., Hassanli, A., Myers, B., Chand, G., 2020. Evaluation of deficit irrigation and water quality on production and water productivity of tomato in greenhouse. *Agric.* 10, 1–18. <https://doi.org/10.3390/agriculture10070297>
- Chen, Y., Banin, A., Borochovitch, A., 1983. Effect of potassium on soil structure in relation to hydraulic conductivity. *Geoderma* 30, 135–147. [https://doi.org/10.1016/0016-7061\(83\)90061-7](https://doi.org/10.1016/0016-7061(83)90061-7)
- Cuevas, J., Daliakopoulos, I.N., Del Moral, F., Hueso, J.J., Tsanis, I.K., 2019. A review of soil-improving cropping systems for soil salinization. *Agronomy* 9, 1–22. <https://doi.org/10.3390/agronomy9060295>
- Dasberg, S., Hopmans, J.W., 1992. Time Domain Reflectometry Calibration for Uniformly and Nonuniformly Wetted Sandy and Clayey Loam Soils. *Soil Sci. Soc. Am. J.* 56, 1341–1345. <https://doi.org/10.2136/sssaj1992.03615995005600050002x>
- Dikinya, O., Areola, O., 2010. Comparative analysis of heavy metal concentration in secondary treated wastewater irrigated soils cultivated by different crops. *Int. J. Environ. Sci. Technol.* 7, 337–346. <https://doi.org/10.1007/BF03326143>
- El-Farhan, A.H. ; Pritts, M.P., 1997. Water requirements and water stress in strawberry. *Adv. Strawb. Res.* 16:5–12.
- Farahani, E., Emami, H., Fotovat, A., Khorassani, R., Keller, T., 2020. Soil available water and plant growth in relation to K:Na ratio. *Geoderma* 363, 114173. <https://doi.org/10.1016/j.geoderma.2020.114173>
- Gardner, W.R., Mayhugh, M.S., Goertzen, J.O., Bower, C.A., 1959. Effect of electrolyte concentration and exchangeable sodium percentage on diffusivity of water in soils. *Soil Sci.* 88, 270–274.

- Gleick, P.H., Heberger, M., 2014. Water conflict chronology. *World's Water Bienn. Rep. Freshw. Resour.* 173–219.
- Hagenvoort, J., Ortega-Reig, M., Botella, S., García, C., de Luis, A., Palau-Salvador, G., 2019. Reusing treated waste-water from a circular economy perspective—the case of the real Acequia de Moncada in Valencia (Spain). *Water* 11, 1830.
- Hailu, B., Mehari, H., 2021. Impacts of Soil Salinity/Sodicity on Soil-Water Relations and Plant Growth in Dry Land Areas: A Review. *J. Nat. Sci. Res.* 12, 1–10.  
<https://doi.org/10.7176/jnsr/12-3-01>
- Haj-Amor, Z., Araya, T., Kim, D.G., Bouri, S., Lee, J., Ghiloufi, W., Yang, Y., Kang, H., Jhariya, M.K., Banerjee, A., Lal, R., 2022. Soil salinity and its associated effects on soil microorganisms, greenhouse gas emissions, crop yield, biodiversity and desertification: A review. *Sci. Total Environ.* 843. <https://doi.org/10.1016/j.scitotenv.2022.156946>
- Hanak, E., 2011. *Managing California's water: from conflict to reconciliation.* Public Policy Instit. CA.
- Hashem, M.S., Qi, X., 2021. Treated Wastewater Irrigation — A Review 1–37.
- Hillel, D., 1998. *Environmental Soil Physics* Academic Press. San Diego, CA.
- Hou, D., Bolan, N.S., Tsang, D.C.W., Kirkham, M.B., O'Connor, D., 2020. Sustainable soil use and management: An interdisciplinary and systematic approach. *Sci. Total Environ.* 729, 138961. <https://doi.org/10.1016/j.scitotenv.2020.138961>
- Jahantigh, M., 2008. Impact of recycled wastewater irrigation on soil chemical properties in an arid region. *Pakistan J. Biol. Sci.* 11(18), 2264-2268.
- Jaramillo, M.F., Restrepo, I., 2017. Wastewater reuse in agriculture: A review about its limitations and benefits. *Sustain.* 9. <https://doi.org/10.3390/su9101734>
- Jeong, H., Bhattarai, R., Adamowski, J., Yu, D.J., 2020. Insights from socio-hydrological modeling to design sustainable wastewater reuse strategies for agriculture at the watershed scale. *Agric. Water Manag.* 231, 105983. <https://doi.org/10.1016/j.agwat.2019.105983>
- Kadir, S., Carey, E., Ennahli, S., 2006. Influence of high tunnel and field conditions on strawberry growth and development. *HortScience* 41, 329–335.  
<https://doi.org/10.21273/hortsci.41.2.329>
- Klay, S., Charef, A., Ayed, L., Houman, B., Rezugui, F., 2010. Effect of irrigation with treated wastewater on geochemical properties (saltiness, C, N and heavy metals) of isohumic soils (Zaouit Sousse perimeter, Oriental Tunisia). *Desalination* 253, 180–187.  
<https://doi.org/10.1016/j.desal.2009.10.019>
- Lagerwerff, J. V., Brower, D.L., 1972. Exchange Adsorption of Trace Quantities of Cadmium in Soils Treated with Chlorides of Aluminum, Calcium and Sodium. *Soil Sci. Soc. Am. J.* 36, 734–737. <https://doi.org/10.2136/sssaj1972.03615995003600050017x>
- Lahlou, F., zahra, Mackey, H.R., McKay, G., Onwusogh, U., Al-Ansari, T., 2020. Water planning framework for alfalfa fields using treated wastewater fertigation in Qatar: An energy-water-food nexus approach. *Comput. Chem. Eng.* 141, 106999.  
<https://doi.org/10.1016/j.compchemeng.2020.106999>
- LaSalle, C., 2018. Recycled Water and High TDS. 33rd Annu. WaterReuse Symp. Austin, TX, Sept. 9-12.
- Marchuk, A., Rengasamy, P., McNeill, A., 2013. Influence of organic matter, clay mineralogy, and pH on the effects of CROSS on soil structure is related to the zeta potential of the dispersed clay. *Soil Res.* 51, 34–40. <https://doi.org/10.1071/SR13012>
- Martin, J.P., Richards, S.J., 1959. Influence of Exchangeable Hydrogen and Calcium, and of

- Sodium, Potassium and Ammonium at Different Hydrogen Levels on Certain Physical Properties of Soils. *Soil Sci. Soc. Am. J.* 23, 335–338.  
<https://doi.org/10.2136/sssaj1959.03615995002300050010x>
- McNeal, B.L., Coleman, N.T., 1966. Effect of solution composition on soil hydraulic conductivity. *Soil Sci. Soc. Am. J.* 30, 308–312.
- Patrignani, A., 2020. andres-patrignani/foilage: Foliage (Version v1.0). Zenodo.
- Perroux, K.M., White, I., 1988. Designs for disc permeameters. *Soil Sci. Soc. Am. J.* 52, 1205–1215.
- Pettygrove, G.S., Asano, T., 1985. Irrigation with reclaimed municipal wastewater. Univ. of California.
- Quirk, J.P., Schofield, R.K., 1955. The effect of electrolyte concentration on soil permeability. *J. Soil Sci.* 6, 163–178.
- Ravina, I., 1973. The mechanical and physical behavior of Ca-clay soil and K-clay soil. *Phys. Asp. soil water salts Ecosyst.* 131–140.
- Reeve, R.C., Bower, C.A., Brooks, R.H., Gschwend, F.B., 1954. A Comparison of the Effects of Exchangeable Sodium and Potassium upon the Physical Condition of Soils. *Soil Sci. Soc. Am. J.* 18, 130–132. <https://doi.org/10.2136/sssaj1954.03615995001800020004x>
- Rengasamy, P., 2018. Irrigation Water Quality and Soil Structural Stability: A Perspective with Some New Insights. *Agronomy* 8, 1–13. <https://doi.org/10.3390/agronomy8050072>
- Rengasamy, P., 2010. Soil processes affecting crop production in salt-affected soils. *Funct. Plant Biol.* 37, 613–620. <https://doi.org/10.1071/FP09249>
- Rengasamy, P., Marchuk, A., 2011. Cation ratio of soil structural stability (CROSS). *Soil Res.* 49, 280–285. <https://doi.org/10.1071/SR10105>
- Rhoades, J.D., 1982. Soluble salts.--p. 167-179. En: *Methods of soil analysis: part 2; chemical and microbiological ....*
- Richards, L.A., 1954. Diagnosis and improvement of saline and alkali soils. (Vol. 78, No. 2, p. 154). *LWW.* 18, 348.
- Scholl, P., Leitner, D., Kammerer, G., Loiskandl, W., Kaul, H.P., Bodner, G., 2014. Root induced changes of effective 1D hydraulic properties in a soil column. *Plant Soil* 381, 193–213. <https://doi.org/10.1007/s11104-014-2121-x>
- Smiles, D.E., Smith, C.J., 2004. A survey of the cation content of piggery effluents and some consequences of their use to irrigate soils. *Soil Res.* 42, 231–246.
- Smith, C.J., Oster, J.D., Sposito, G., 2015. Potassium and magnesium in irrigation water quality assessment. *Agric. Water Manag.* 157, 59–64. <https://doi.org/10.1016/j.agwat.2014.09.003>
- Sposito, G., Oster, J.D., Smith, C.J., Assouline, S., 2016. Assessing soil permeability impacts from irrigation with marginal-quality waters. *CAB Rev. Perspect. Agric. Vet. Sci. Nutr. Nat. Resour.* 11, 1–7. <https://doi.org/10.1079/PAVSNNR201611015>
- Thaker, P.N., Brahmabhatt, N., Shah, K., 2021. A review: Impact of soil salinity on ecological, agricultural, and socio-economic concerns. *Int. J. Adv. Res.* 9, 979–986.
- UNICEF, WHO, 2022. World Health Organization.
- USDA-NRCS, 2013. Irrigation National Engineering Handbook Chapter 7.
- Velasco, E.S., 2013. Scanning Electron Microscope (SEM) as a means to determine dispersibility. Iowa State Univ. Ames, IA, USA.
- Vergine, P., Salerno, C., Libutti, A., Beneduce, L., Gatta, G., Berardi, G., Pollice, A., 2017. Closing the water cycle in the agro-industrial sector by reusing treated wastewater for irrigation. *J. Clean. Prod.* 164, 587–596. <https://doi.org/10.1016/j.jclepro.2017.06.239>

- Wallender, W., Tanji, K., 1990. Agricultural salinity assessment and management, 2nd ed. American Society of Civil Engineers (Vol. 54, pp. 413-415).
- Xu, J., Wu, L., Chang, A.C., Zhang, Y., 2010. Impact of long-term reclaimed wastewater irrigation on agricultural soils: A preliminary assessment. *J. Hazard. Mater.* 183, 780–786. <https://doi.org/10.1016/j.jhazmat.2010.07.094>
- Yang, H., Rahardjo, H., Wibawa, B., Leong, E.-C., 2004. A soil column apparatus for laboratory infiltration study. *Geotech. Test. J.* 27, 347–355.

## Appendix

The section is intended to show the photographs captured during the soil column and greenhouse experiments. These images are valuable in understanding the setup of both the column and greenhouse experiments. Furthermore, they have the potential to function as educational aids for students when teaching classes related to the subject matter of this study. Additionally, they could serve as demonstration content for books and other literature.

Soil column experiment:



Figure: Soil preparation site in the University of California Davis (UCDavis) greenhouse facility.

The soil was prepared for both column and greenhouse experiment.



Figure: Bottom-up pre-saturation of the soil column with tap water before running the infiltration experiment.



Figure: Running the infiltration experiment using the wooding infiltrometer and collection of the drainage water into the buckets that are in the ground.



Figure: Screenshot from the blink APP coupled with Blink Camera to live monitor the water level in the wooding infiltrometer to make sure that water does run out. The camera turns to night vision when the lab lights are off.



Figure: Sampling from the soil columns by depth using augur core sampler after conducting the infiltration experiment. The results of the clay dispersion by depth are shown in Chapter 2 Figure 2.7.



Figure: Photograph of the top view of the soil column before (left) and after (right) running the experiment for T0.



Figure: Photograph of the top view of the soil column before (left) and after (right) running the experiment for T1.



Figure: Photograph of the top view of the soil column before (left) and after (right) running the experiment for T2.



Figure: Photograph of the top view of the soil column before (left) and after (right) running the experiment for T3.



Figure: Photograph of the top view of the soil column before (left) and after (right) running the experiment for T4.



Figure: Photograph of the top view of the soil column before (left) and after (right) running the experiment for T5.



Figure: Photograph of the top view of the soil column before (left) and after (right) running the experiment for T6.



Figure: Photograph of the top view of the soil column before (left) and after (right) running the experiment for T7.



Figure: Photograph of the top view of the soil column before (left) and after (right) running the experiment for T8.



Figure: Photograph of the top view of the soil column before (left) and after (right) running the experiment for T9.

Greenhouse experiment:

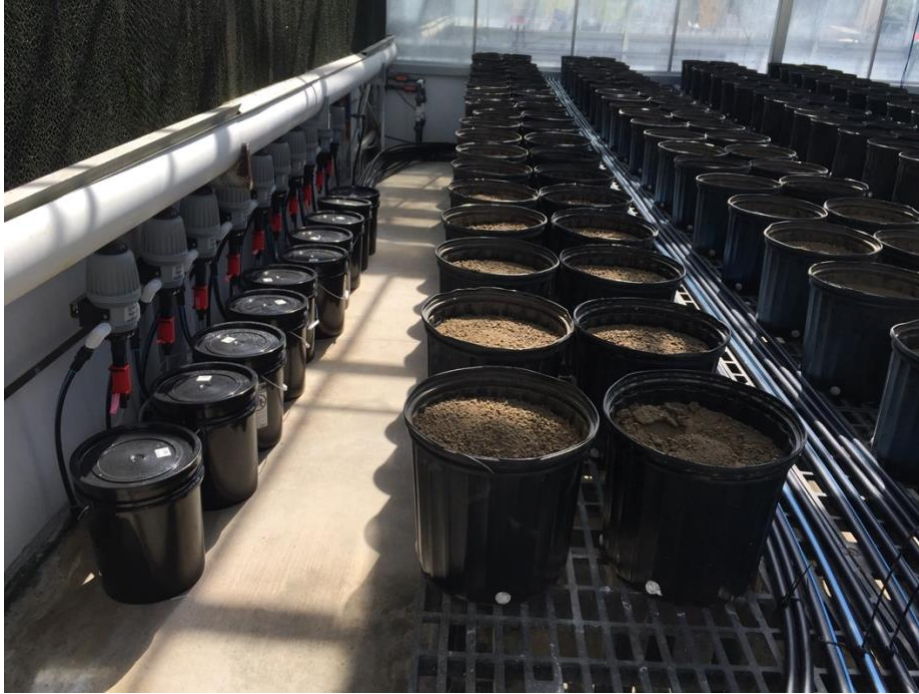


Figure: Pots filled with soil. In total 176 pots were prepared for 11 treatments and 4 blocks. The 5 gallon buckets in the ground have the concentrated form of the treatment and RiteMix Injectors were connected from the buckets to the irrigation line to provide irrigation water with conductivity of 1.5 dS/m.



Figure: A strawberry plant on its second week. The small grains are the slow-release fertilizer (Osmocote Plus 15-9-12) to promote plant growth.



Figure: the greenhouse experiment with the strawberry plants. We can see here the method of leachate collection from the pots. The leachate was collected for each treatment from three

different pots. The analysis of the leachate is shown in the chapter 4 of this document in Figure 4.2, 4.3 and 4.4.



Figure: Example of the output of the Foliage tool that was used to estimate weekly plant cover.

The results are presented in Chapter 4 in Figure 4.5.



Figure: Strawberry plants in the pots with the fruits before harvesting.



Figure: Infiltration experiment conducted over the soil in pots after terminating the greenhouse experiment. The results are presented in Chapter 3 in Figure 3.5.



Figure: Example of the output of the Foliage tool that was used to estimate the plant cover at the end of the experiment before harvesting the whole plant. The results are presented in Chapter 4 in Figure 4.10b.